Interaction of Amaranth with Some Alkyltrimethylammonium Salts: A Coacervation Phenomenon

B. W. BARRY▲ and G. F. J. RUSSELL*

Abstract □ The interaction of some commercial alkyltrimethylammonium bromides with amaranth BPC was investigated by an extraction technique, surface tension, viscosity, light scattering, microscopy, microelectrophoresis, spectroscopy, and phase studies. Interaction in aqueous solution was shown to be a coacervation phenomenon, and results were interpreted using general coacervation theories.

Keyphrases □ Alkyltrimethylammonium salts—coacervation with amaranth □ Amaranth—coacervation with alkyltrimethylammonium salts □ Coacervation, amaranth–alkyltrimethylammonium salts—determination by extraction, surface tension, viscosity, light scattering, microscopy, spectroscopy, microelectrophoresis, phase studies

The compatibility of dyes with other substances is an important factor to consider when a pharmacist formulates a product. The number of dyes permitted in foods and drugs decreases as more is learned about their properties, and it is desirable to increase knowledge of those remaining, especially regarding compatibility with other pharmaceuticals.

Surfactants are used extensively in pharmacy to prepare, for example, emulsions and solubilized preparations of such drugs as the oil-soluble vitamins and steroids (1). Since such liquid preparations may contain a dye, it is desirable to investigate any interaction between dye and surfactant. The interaction of surfactants with dyes was examined by several workers (2–13) and was used extensively in the determination of surfactant concentration and CMC, although the nature of the species formed was not fully resolved. The unusual behavior of these complexes was explained by ion pairs (14, 15), surfactant–dye micellar species (16), and insoluble complex salts of the type $(\text{surfactant}_m\text{–dye}_n)_x$, where m is much greater than n but less than the micellar amount (17). Mukerjee and Mysels (11) postulated that a water-insoluble salt formed a stable suspension in the presence of more than stoichiometric amounts of surfactant by inducing the formation of mixed micelles at concentrations considerably below the CMC.

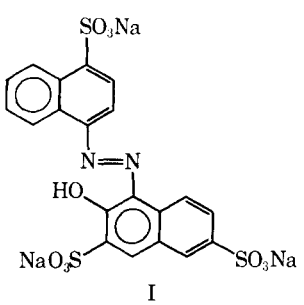

I

Numerous publications deal with indicator dye–surfactant interactions, but little information is available on the compatibility of permitted food dyes and long-chain quaternary ammonium salts used in pharmaceuticals. It is possible that dye–surfactant interactions and the mode of solubilization of such complexes in surfactant micelles will influence the stability of dye solutions to heat and light. A knowledge of the physicochemical aspects of such interactions is, therefore, necessary before commencing stability studies. In this paper, the interaction of amaranth (I) with some long-chain quaternary ammonium salts is investigated by surface tension, viscosity, light scattering, microscopy, microelectrophoresis, spectroscopy, phase studies, and an extraction technique.

EXPERIMENTAL

Materials—The following commercial alkyltrimethylammonium bromides[1] were used: octadecyltrimethylammonium bromide, hexadecyltrimethylammonium bromide, tetradecyltrimethylammonium bromide, dodecyltrimethylammonium bromide, and cetrimide[2] BP (a commercially available mixture of alkyltrimethylammonium bromides complying with the specification of the British Pharmacopoeia). Alkyl bromides[3] were used to identify GC peaks. A commercial sample of amaranth[4], trisodium 2-hydroxy-1-(4-sulfo-1-naphthaleneazo)naphthalene-3:6-disulfonate (complying with the specification of the British Pharmaceutical Codex, 1954), was found to be 93.3% pure with respect to the dry weight.

Clark and Lub's buffers were used for pH values 1.0–10.0. Teorell and Stenhagen's citrate–phosphate–borate buffer and 0.1 N NaOH were employed for pH values above 10.0.

All other chemicals were of analytical grade; water, doubly distilled from an all-glass still, of specific conductance not greater than 1.2×10^{-6} ohm^{-1} cm.^{-1} was used.

GLC—A flame-ionization gas chromatograph[5] was used. The column, similar to that used by Metcalfe (18), was of stainless steel tubing, 0.32 cm. o.d. and 2 m. in length. The packing consisted of Apiezon L-KOH on acid-washed 60–80 mesh Chromosorb W in the ratio 20:10:70. Nitrogen was used as the carrier gas at a flow rate of 27 ml. min.^{-1}, with an oven temperature of 232° and an injection temperature of 250°. The injection solvent was isopropyl alcohol. Peak areas were measured by electronic integration[6]. Further details were published elsewhere (19, 20).

[1] Schuchardt München, München, West Germany.
[2] Compass Chemicals Ltd., London, England.
[3] 1-Bromododecane, B.D.H. Chemicals Ltd., Poole, England; 1-bromotetradecane, Ralph N. Emanuel Ltd., Alperton, England; and 1-bromohexadecane, Hopkins and Williams Ltd., Chadwell Heath, England.
[4] D. F. Anstead Ltd., Billericay, England.
[5] Perkin-Elmer F11.
[6] Integrator type 165A, Gas Chromatograph Ltd., Maidenhead, England.

Traces were obtained for all the alkyltrimethylammonium bromides and the parent alkyl bromides.

Amaranth Spectra—Spectra of aqueous solutions of amaranth (0.03 mmole/l.) were determined over the pH range 2.6–13. The buffer solutions used were already described, and pH was checked at room temperature[7].

Potentiometric titration confirmed that the sulfonate groups were completely dissociated at all pH values used, since the pKa value was less than 1.5. Donbrow (21) reported similar results.

Determination of CMC—CMC's in water were determined at 25 ± 0.02° by the conductivity and surface tension methods[8]. Readings were taken until two consecutive results within 0.2 dyne cm.$^{-1}$ were obtained.

Stoichiometry of Dye–Surfactant Interaction—When an aqueous solution of amaranth was added to an aqueous solution of a quaternary ammonium salt, a gelatinous red precipitate formed due to interaction between ions of opposite charge. The stoichiometry of this dye–surfactant complex was determined by adapting the method of Few and Ottewill (22), in which a water-soluble dye reacts with an oppositely charged long-chain ion and the resulting water-insoluble complex is completely transferred to an immiscible organic solvent in which the dye is insoluble. As the complexes formed between amaranth and the quaternary ammonium compounds were adsorbed by glass, the method was modified as follows. Five milliliters of 0.01% (14.45 mmoles/l.) aqueous dye solution and 5 ml. of aqueous surfactant solution below the CMC (of concentration between 0.025 and 0.15 mmole/l.) were pipeted into a glass-stoppered centrifuge tube, and 1 ml. of 2% boric acid in ethanol was added (12). Chloroform (5 ml.) was added and the tubes were shaken for 2 min. to extract the dye–surfactant complex. The tubes were centrifuged, samples were removed, and the absorbance of the chloroform layer was read at 522 nm. ($\lambda_{max.}$). Further extractions were carried out as necessary until transference was completed and the absorbance stopped rising. The concentrations of reactants ensured that excess dye was present so that all surfactant was complexed and transferred to the chloroform. In a second series, dye and surfactant solutions were equilibrated using an excess of the latter (50 mmoles/l. of surfactant and concentrations of dye less than 2.89 mmoles/l.) so that complete transfer of dye occurred. A plot of absorbance at $\lambda_{max.}$ (522 nm.) *versus* dye concentration obeyed the Beer–Lambert law and was used to determine dye concentrations in chloroform. The procedure was applied to all five commercial quaternary ammonium salts at pH values from 4.8 to 12.8.

To substantiate the stoichiometry of the complexes, they were prepared by mixing aqueous solutions of 0.05 *M* dye and 0.13 *M* surfactant, *i.e.*, a slight excess of dye. For each quaternary ammonium salt, a red gel-like precipitate formed which became more viscous on equilibrating the solutions for 12 hr. Because of their consistencies, it was not possible to centrifuge or filter the resulting complexes. They were extracted with 30-ml. aliquots of chloroform, which were mixed with anhydrous sodium sulfate to clear water droplets, filtered through glass wool, and evaporated to dryness on a watchglass over a water bath. Some crystalline complexes were presented for elemental analysis.

Characterization of Complexes—The complexes were examined for appearance and qualitative solubility in various solvents. The UV, visible, and IR spectra were examined[9]. Potassium bromide disks were prepared for IR work. TLC was applied to determine R_f values and to separate components of the complexes. Many eluting solvents and adsorbents were tried, the best being: (*a*) *n*-propanol–ethyl acetate–water (6:1:3) using cellulose MN 300G (0.25 mm. thickness) as adsorbent, and (*b*) *n*-butanol–glacial acetic acid–water (50:15:43) using silica gel G and water (0.25 mm. thickness) as adsorbent. The plates were sprayed with Dragendorff's reagent after development to render the quaternary ammonium group visible.

The complexes were examined in normal light and between crossed polars at ×400[10].

Each complex was heated on a Kofler hot-stage on the microscope. Crystals were viewed through crossed polars and changes were noted as the temperature was slowly raised and then as the melt cooled.

Solubilization of Complexes in Excess Surfactant—Riegelman *et al.* (23) developed a method for determining the mode of solubilization of a substance in a micellar solution. The method is based on the fact that the UV spectrum of most compounds is sensitive to changes in the environment, especially to changes in the dielectric constant. Since micelles possess regions of different polarity, the UV spectrum of the dye–surfactant complex when solubilized depends on the position it occupies in the micelle. The UV spectra were determined initially on an automatic reading spectrophotometer[11], and $\lambda_{max.}$ and inflections then were measured accurately[12]. The position of $\lambda_{max.}$ and the degree of fine structure were determined for the complexes in water, absolute ethanol, *n*-pentanol, chloroform, and an aqueous solution of the quaternary ammonium salt above the CMC.

Surface Tension Measurements on Solutions of Dye–Surfactant Complexes—These were made using a tensiometer[13] with a platinum ring. Fresh aqueous solutions of the dye–surfactant complexes were placed in a temperature-controlled water bath, and readings were taken until two consecutive results within 0.2 dyne cm.$^{-1}$ were obtained. All solutions were visually clear except some of the tetradecyltrimethylammonium bromide– and dodecyltrimethylammonium bromide–dye complexes which were slightly turbid. Surface tension–concentration curves were also obtained for amaranth, dodecyltrimethylammonium bromide, and hexadecyltrimethylammonium bromide in the concentration range of the complexes.

Phase Study Titrations—A 10-ml. aliquot of a 1-mmole/l. aqueous dye solution was titrated against a suitable concentration of surfactant in 1 mmole/l. aqueous dye solution so that during the titration the concentration of dye remained the same. A turbid solution formed as soon as the dye–surfactant solution was added to the dye solution. The end-point, which was quite distinct, was recorded when the turbidity disappeared. The ratio of surfactant to dye in the final clear solution was calculated. The effects of dye concentration (0.5–8 mmoles/l.) and surfactant concentration (5–30 mmoles/l.) on this ratio were examined. At a concentration of dye in excess of 8 mmoles/l., viscous solutions formed which prevented accurate determinations. When the titration procedure was reversed, *i.e.*, a 10-ml. aliquot of dye–surfactant solution was titrated against dye solution until turbidity commenced, the ratio of surfactant to dye in the final solution was unaltered. Titrations were performed at room temperature (~22°) with cetrimide, dodecyltrimethylammonium bromide, tetradecyltrimethylammonium bromide, and hexadecyltrimethylammonium bromide.

The effects of temperature and sodium chloride concentration on the titration of cetrimide–dye solutions were also determined.

Heating Experiments—For surfactant concentrations above the CMC, aqueous solutions containing 1.5 mmoles/l. of dye and varying concentrations of each surfactant were heated slowly with stirring, and evaporation losses were compensated for by adding water. The temperature was recorded when turbidity commenced. Turbidity occurred over a 3° range for the higher homologs but was more precise for the lower homologs.

Determinations below the CMC were made with aqueous solutions containing 0.15 mmole/l. dye and varying concentrations of surfactant.

To determine the effect of dye concentration on the turbidity temperature, the procedure was repeated for dodecyltrimethylammonium bromide– and hexadecyltrimethylammonium bromide–dye solutions above and below the CMC. Concentrations of dye used were: dodecyltrimethylammonium bromide (above CMC)—0.75, 1.00, 1.50, and 2.00 mmoles/l.; dodecyltrimethylammonium bromide (below CMC)—0.05, 0.075, 0.10, and 0.15 mmole/l.; hexadecyltrimethylammonium bromide (above CMC)—0.29, 0.75, 1.00, 1.50, and 2.00 mmoles/l.; and hexadecyltrimethylammonium bromide (below CMC)—0.072, 0.10, 0.15, and 0.175 mmole/l.

The effect on the turbidity phenomenon of concentrations of different salts was investigated. Salts used were sodium chloride, sodium sulfate, sodium citrate, and calcium chloride; *i.e.*, the valency of the cation and anion were varied. A suitable salt with a trivalent

[7] With an E.I.L. direct reading pH meter, model 23A, using glass electrodes.

[8] Conductivity measurements were made with a Wayne Kerr Universal Bridge B641 with a source frequency of 1592 Hz., using a Philips midget conductivity measuring cell PW 9512/01 with blackened platinum electrodes. Surface tension measurements were made using a Du Noüy tensiometer with a platinum ring.

[9] Using Unicam SP.800 and Perkin-Elmer 257 spectrophotometers.

[10] Using a Vickers polarizing microscope.

[11] Unicam SP.800.

[12] Using a Uvispek spectrophotometer.

[13] Du Noüy.

Table I—Analysis of Alkyltrimethylammonium Bromides by GLC; Percentage Homolog Calculated on a Dry Weight Basis

Constituents Present	Commercial Alkyltrimethylammonium Bromides					Retention Time of Peak, min.
	Octadecyl-	Hexadecyl-	Tetradecyl-	Dodecyl-	Cetrimide	
Octadecyltrimethylammonium bromide	90.7	2.0	—	—	—	64.3
Octadecyl bromide	1.0	—	—	—	—	55.5
Heptadecyltrimethylammonium bromide	—	0.7	—	—	—	—
Hexadecyltrimethylammonium bromide	2.7	89.5	3.8	3.4	7.1	33.5
1-Bromohexadecane	—	1.5	—	—	(0.2)	26.3
Pentadecyltrimethylammonium bromide	1.1	1.0	(0.4)[a]	0.8	(0.2)	22.5
Tetradecyltrimethylammonium bromide	2.6	1.9	91.3	21.4	67.9	16.5
1-Bromotetradecane	—	—	1.4	—	1.6	13.8
Tridecyltrimethylammonium bromide	—	1.8	1.1	(0.4)	0.8	11.0
Dodecyltrimethylammonium bromide	2.0	0.9	1.7	71.0	21.9	8.3
1-Bromododecane	—	—	—	0.6	(0.3)	6.3
Undecyltrimethylammonium bromide	—	—	0.6	(0.3)	0.5	5.5
Decyltrimethylammonium bromide	—	1.2	—	2.2	0.5	4.0

[a] Data in parentheses represent estimated values.

cation was not found; salts such as $FeCl_3$ form their own sols which react with the dye molecule.

Viscosity Measurements[14]—The effect of surfactant concentration (above and below the nominal CMC of the surfactant) at dye concentrations of 1.5 and 0.15 mmoles/l., respectively, on the viscosity of dodecyltrimethylammonium bromide–, tetradecyltrimethylammonium bromide–, and hexadecyltrimethylammonium bromide–dye solutions was determined. Measurements were initiated on aqueous solutions and in 0.1 *N* NaOH at pH 12.0. The effect of dye concentration on the viscosity of aqueous cetrimide solutions above (10 and 20 mmoles/l.) and below (2 and 3 mmoles/l.) the CMC was also determined.

Light-Scattering Measurements—It was considered that light-scattering measurements on aqueous solutions of the isolated dye–surfactant complexes would indicate the presence of micelles and also give an approximate apparent micellar molecular weight. Turbidities were measured at 25 ± 0.1° with a photometer[15] using unpolarized incident light of wavelength 436 nm. and a 40 × 40-mm. semioctagonal dissymmetry cell. The photometer was calibrated against an opal glass diffuser as a reference standard, and the observed Rayleigh ratio for water was found to be 2.77×10^{-6} $cm.^{-1}$, which is in good agreement with previously reported values (24). Initially, solutions were filtered into the cell through a washed Millipore cellulose membrane filter of pore size 0.1 μm., but at low concentrations some color was removed from the solution. It was suspected that this was due to the formation of a fine suspension or coacervate of the complex in aqueous solution at low concentrations, which was removed from solution by the membrane filter. The technique was, therefore, adapted so that the concentration at which the suspension or coacervate formed could be determined. A concentrated solution of dye–surfactant complex (which was not coacervated) was filtered into the cell through a membrane filter and diluted with water (also filtered directly into the cell) to give appropriate concentrations for light-scattering measurements. The concentrations of these solutions were determined by withdrawing a small sample with a syringe, measuring the absorbance at $\lambda_{max.}$, and reading from a Beer–Lambert curve; straight-line Beer–Lambert plots were obtained for all complexes. No corrections to the turbidity values due to color absorption were required since absorbances were low.

Dissymmetries, Z (I_{45}/I_{135}, where I_{45} and I_{135} are the intensities of scattered light at 45 and 135°, respectively), as well as turbidities were determined. Light scattering of dye solution alone was negligible. The procedure was satisfactory for the octadecyltrimethylammonium bromide– and hexadecyltrimethylammonium bromide–dye complexes, but problems were encountered with the other complexes because of rapid coacervation on standing. This was followed with a dual photomultiplier arrangement so that readings at 0 and 90° could be taken simultaneously. This was necessary to follow the rapid coacervation with time of the short-chain surfactant–dye complexes.

Microscopic Examination of Turbid Solutions—To elucidate the nature of the turbid solutions produced when dilute aqueous dye and surfactant solutions are mixed, these solutions were examined in normal light using a polarizing microscope[16] with a camera attachment. The turbidity produced on heating clear aqueous solutions of dye and surfactant (see *Heating Experiments*) was investigated microscopically by warming these solutions on a Kofler hot-stage; the slow development of turbidity in aqueous solutions of extracted crystalline complexes was also examined (see section on *Light Scattering*). It became clear from the experiments that turbidity was not due to a fine precipitate but that it was a *coacervation* phenomenon.

Microelectrophoresis—To investigate the charge and movement of the coacervate droplets in an electric field, a microelectrophoresis apparatus of the "flat cell" type similar to that described by Abramson *et al.* (25) was used. The cell[17], 2 cm. wide and 0.5 cm. deep, was used in the horizontal position clamped to a Kofler hot-stage on a microscope. The electrodes were zinc/zinc sulfate[18]. Since only qualitative results were of interest in this investigation, an accurate value for the electric field strength in the cell was not required. In all investigations the microscope was focused on the stationary layer of the solution in the cell according to the recommendation of

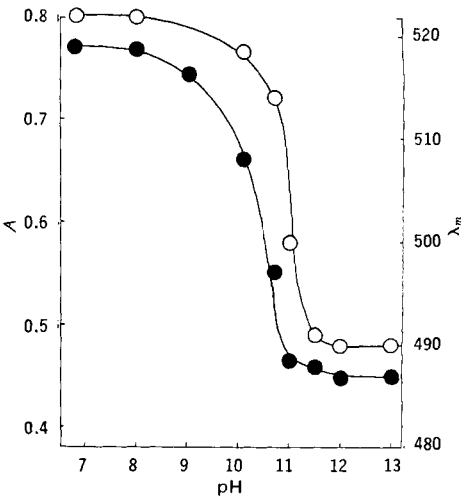

Figure 1—*Influence of pH on the absorbance* (A) *of aqueous amaranth solution* (*0.03 mmole/l.*) *at* $\lambda_{max.}$, *and the variation of* $\lambda_{max.}$ *with pH. Key:* ○, $\lambda_{max.}$ versus *pH; and* ●, *absorbance* (A) versus *pH.*

[14] Viscosities were determined with a British Standard Type A capillary viscometer at 25 ± 0.02° using the procedure of the British Standard Specification, 188:1957.

[15] Brice-Phoenix Universal light-scattering photometer, supplied by Techmation Ltd., London, England.

[16] Vickers.

[17] Constructed by Linskey Brothers, Kings Cross, London, England.

[18] The power source was a Shandon Vokam power supply unit, type 2541; Shandon Scientific Co. Ltd., London, England.

Table II—Effect of pH on Maxima in the UV Spectrum of an Aqueous Solution of Amaranth

pH	Wavelengths, nm.					
4.8–10.1	333	322[a]	306[a]	(290)	279	240[a]
10.8	355	(305)[b]	(280)	247	—	—
12.0	358	(300)	(278)	247	—	—
12.8	358	(300)	(278)	247	—	—

[a] An inflection. [b] Numbers in parentheses represent a shoulder.

Smoluchowski (26). Systems were examined in excess surfactant, excess dye, and at the surfactant–dye ratio of 3:1.

Approximate Analysis of Coacervated System—Aqueous solutions of dye (33.3 mmoles/l.) and dodecyltrimethylammonium bromide (100 mmoles/l.) were mixed, and the coacervated system was filtered through a washed Millipore filter (0.1 μm.). Then 50 ml. of the filtered solution was evaporated to dryness and made up to 25 ml. with isopropyl alcohol. This solution was analyzed for surfactant content by GLC as described previously. Two microliters of this solution was injected onto the GLC column, and the number of integrator units and sensitivity scale reading were noted. The procedure was repeated with dodecyltrimethylammonium bromide solution alone. A comparison of integrator units enabled the percentage dodecyltrimethylammonium bromide retained in the coacervate to be calculated. The dye present in the filtrate was determined by diluting the filtrate ×10 with water and reading the absorbance in 1.0-cm. cells at 522 nm.

RESULTS

For each compound subjected to GC, a sharp major peak was obtained together with several minor peaks. By plotting alkyl chain length *versus* the logarithm of the retention time, these minor peaks were identified as due to homologous impurities and the parent alkyl bromides. Table I shows the composition of each long-chain paraffin salt and the appropriate retention times.

The effect of pH on the visible absorption spectrum of amaranth can be seen from Fig. 1 to give a sigmoidal curve. The variation of $\lambda_{max.}$ with pH is also sigmoidal, the wavelength changing from 522 to 490 nm. over approximately the same range of pH as absorbance changes.

The wavelengths of peaks at different pH's observed in the UV region are given in Table II.

At pH values 4.8–10.1, a shoulder was observed at 240 nm. which gradually became an inflection as the pH of the solution was increased above this range; at pH 10.8, it was a definite peak at 247 nm. The peak at 279 nm. was gradually depressed and that at 333 nm. showed a bathochromic shift to 358 nm. with increasing pH.

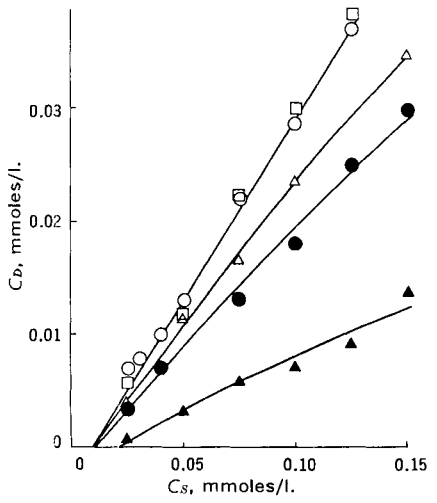

Figure 2—*Plot of concentration of dye* (C_D, *millimoles per liter*) versus *concentration of surfactant* (C_S, *millimoles per liter*) *after one chloroform extraction. Key:* ○, *octadecyltrimethylammonium bromide;* □, *hexadecyltrimethylammonium bromide;* △, *tetradecyltrimethylammonium bromide;* ●, *cetrimide; and* ▲, *dodecyltrimethylammonium bromide.*

Table III—CMC of Alkyltrimethylammonium Bromides at 25°

Surfactant	CMC, mmoles/l. Conductivity	CMC, mmoles/l. Surface Tension
Cetrimide	2.9	3.3
Dodecyltrimethylammonium bromide	5.3	5.2
Tetradecyltrimethylammonium bromide	3.3	3.4
Hexadecyltrimethylammonium bromide	0.82	0.80
Octadecyltrimethylammonium bromide	0.30	0.31

The CMC results from surface tension and conductivity measurements are shown in Table III.

Figure 2 shows the plots of molarity of dye (calculated from absorbance readings) *versus* molarity of surfactant in the chloroform phase after one extraction.

Subsequent extractions of tetradecyltrimethylammonium bromide–dye solutions eventually moved this curve so that it was superimposable on the octadecyltrimethylammonium bromide and hexadecyltrimethylammonium bromide curves. Cetrimide and dodecyltrimethylammonium bromide complexes containing a high proportion of short-chain homologs, were difficult to extract completely. The effect of varying the pH of the aqueous phase of the most easily extractable complex, that of octadecyltrimethylammonium bromide, can be seen from Fig. 3.

The slope of the curve is unaltered in acid and neutral solutions, but the slope is smaller above a pH of about 10.0. A similar set of curves was obtained for hexadecyltrimethylammonium bromide and, after many extractions, for tetradecyltrimethylammonium bromide. Curves for cetrimide and dodecyltrimethylammonium bromide were obtained at acid and neutral pH only because so little of the dye–surfactant complex could be extracted at alkaline pH. Other organic solvents tried were benzene, *n*-pentanol, ethyl acetate, and tetrachloroethane, but none was better than chloroform.

The results of elemental analyses for selected dye–surfactant complexes are given in Table IV. The theoretical values for carbon, hydrogen, and nitrogen were estimated from the analyses of the quaternary ammonium salts given in Table I. The estimated accuracy for C, H, and N is ±0.3, ±0.2, and ±0.3% absolute, respectively.

Complexes obtained from aqueous solution varied from bright red for dodecyltrimethylammonium bromide to dark red for octadecyltrimethylammonium bromide. Octadecyltrimethylammonium bromide– and hexadecyltrimethylammonium bromide–dye complexes obtained at alkaline pH were dark purple.

All complexes were initially slightly soluble in water (solubility decreasing with increasing alkyl chain length) but precipitated on standing for several days. They were very soluble in chloroform, methanol, ethanol, acetone, and *n*-pentanol but insoluble in hexane, diethyl ether, and cyclohexane. Of these solvents, amaranth alone is soluble only in water and methanol and is slightly soluble in ethanol;

Table IV—Elemental Analysis of Some Dye–Surfactant Complexes[a]

Surfactant	pH at Which Complex Was Obtained	Analysis, %	Calc.	Found
Octadecyltrimethylammonium bromide	12.8	C	69.6	70.0
		H	10.5	10.3
		N	4.8	4.5
Octadecyltrimethylammonium bromide	6.8	C	68.0	68.9
		H	9.7	9.9
		N	4.8	4.5
Hexadecyltrimethylammonium bromide	6.8	C	66.3	65.2
		H	9.8	9.8
		N	5.1	4.4
Tetradecyltrimethylammonium bromide	6.8	C	65.1	64.0
		H	9.5	9.4
		N	5.4	4.9

[a] Percentage *S* is not included because the inaccuracy of determination was significant compared to the calculated value.

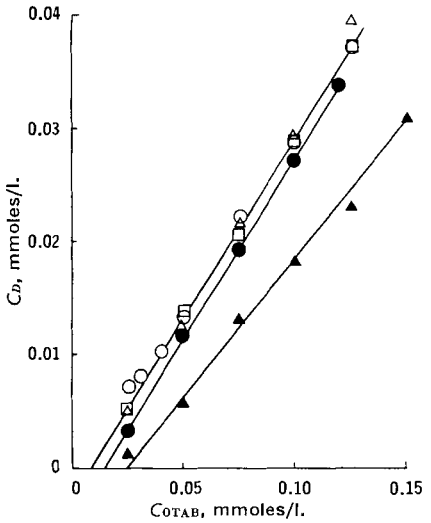

Figure 3—*Effect of pH on the extraction of octadecyltrimethylammonium bromide (OTAB)–dye complex into chloroform;* C_D *is the concentration of dye and* C_{OTAB} *the concentration of surfactant in millimoles per liter. Key:* ○, *water;* △, *pH 4.8;* □, *pH 8.0;* ●, *pH 10.1; and* ▲, *pH 12.8.*

i.e., the dye–surfactant complexes tend to be soluble in less polar solvents than water.

The UV spectra of the complexes in water were similar to that of the dye itself, a small bathochromic shift being observed for the main peak at 333 nm. The peak in the visible region was 522 nm. initially but moved to 528 nm. with time. The IR spectra were identical to those of simple mixtures of dye and surfactant, indicating that no major structural changes had taken place during complexation. This was also shown by the TLC experiments. Both TLC eluting solvents mentioned previously gave satisfactory separation of the dye and quaternary ions of the complexes. The R_f values were as follows: (*a*) *n*-propanol–ethyl acetate–water (6:1:3), dye anion 0.40, quaternary cation 0.96, run time = 195 min., and (*b*) *n*-butanol–glacial acetic acid–water (50:15:43), dye anion 0.39, quaternary cation 0.59. In addition, a faint spot due to a dye impurity was observed with an R_f value of 0.57, run time = 200 min.

When crystals of the complexes were examined microscopically in ordinary light, scattered small circles were visible in a larger red mass. Figure 4 is a photomicrograph of crystals of the tetradecyltrimethylammonium bromide–dye complex obtained at pH 6.8 viewed under polarized light. It can be seen that the complex contains strongly anisotropic circular masses which have the appearance of a "Maltese Cross." Similar observations were made for all dye–surfactant crystals obtained at neutral and alkaline pH. Results of

Figure 4—*Crystals of amaranth–tetradecyltrimethylammonium bromide complex viewed through crossed polars; 1 division = 100 μ.*

Table V—Melting Points of Dye–Surfactant Complexes and Surfactants Alone Using Kofler Hot-Stage

Alkyltrimethylammonium Bromide	pH at Which Complex Was Obtained	Melting Point of Complex	Melting Point of Surfactant
Octadecyl-	6.8	230–235°	218–220°
Octadecyl-	12.8	233–236°	218–220°
Hexadecyl-	6.8	235–238°	222–225°
Hexadecyl-	12.8	220–225°	222–225°
Tetradecyl-	6.8	210–214°	227–229°
Cetrimide	6.8	210–214°	198–200°
Dodecyl-	6.8	210–214°	218–220°

heating each complex on a Kofler hot-stage are presented in Table V. Crystals became completely isotropic at the melting point; on cooling, the melt produced much larger spherulites. Melting points of surfactants alone using the same technique are also given for comparison. The melting point of amaranth was greater than 300°. Crystals of surfactant were slightly anisotropic and tended to be needle shaped. No spherulites were observed, even in the cooled melt.

Table VI indicates the UV spectra of the dye–surfactant complexes obtained at neutral and alkaline pH in various solvent systems.

Figures 5 and 6 show surface tension curves at 25° for dodecyltrimethylammonium bromide–, tetradecyltrimethylammonium bromide–, hexadecyltrimethylammonium bromide–, and octadecyltrimethylammonium bromide–dye complexes of stoichiometry (moles of surfactant to moles of dye) 3:1 and for hexadecyltrimethylammonium bromide– and octadecyltrimethylammonium bromide–dye complexes of stoichiometry 4:1. Plots are also shown for aqueous dye solution and aqueous solutions of dodecyltrimethylammonium bromide and tetradecyltrimethylammonium bromide for comparison. It can be seen that an inflection point is obtained for some complexes, but minima are observed for others. Table VII indicates the approximate inflection point or minima for these complexes, together with a value obtained from light-scattering data.

Results obtained from the phase study titrations in aqueous solution are presented graphically in Fig. 7 as the minimum ratio of surfactant to dye for compatibility *versus* concentration of dye (C_D, millimoles per liter). The area above each curve represents a clear solution (compatibility of dye and surfactant), and the area below each curve represents a turbid solution (incompatibility). The effect of temperature on the minimum ratio of cetrimide to dye for compatibility in solutions containing 1 mmole/l. dye can be seen from

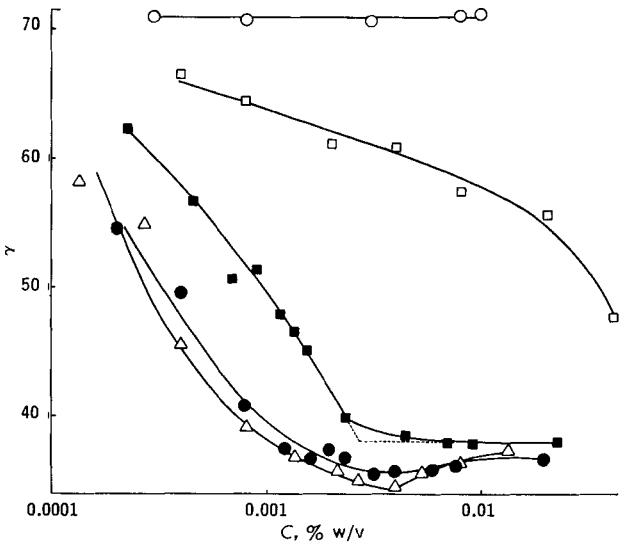

Figure 5—*Plots of surface tension* (γ, *dyne cm.*$^{-1}$) versus *concentration of dye–surfactant complex or tetradecyltrimethylammonium bromide or dye* (C, % *w/v*) *at 25°. Key:* ■, *tetradecyltrimethylammonium bromide–dye (3:1);* ●, *hexadecyltrimethylammonium bromide–dye (3:1);* △, *hexadecyltrimethylammonium bromide–dye (4:1);* □, *tetradecyltrimethylammonium bromide only; and* ○, *dye only.*

Table VI—Maxima (nm.) in the UV and Visible Spectra of Dye–Surfactant Complexes in Various Solvent Systems

Surfactant	pH at Which Complex Was Obtained	Solvent	UV Region							Visible Region
Octadecyltrimethylammonium bromide	6.8	Water	336	327[a]	310[a]	(295)[b]	280[a]	240[a]	—	522
		Ethanol	333.5	325[a]	307[a]	(293)	281	240[a]	—	524
		n-Pentanol	334	325[a]	308[a]	(294)	(282)	240[a]	—	526
		Chloroform	337	327[a]	310	(295)	283	—	—	526
		Aqueous surfactant above the CMC	333.5	326[a]	307[a]	(293)	281	240[a]	—	524
Octadecyltrimethylammonium bromide	12.8	Water	365	336[a]	(295)	(275)	240[a]	—	—	522
		Ethanol	360	333.5	324[a]	306	(295)	276.5[a]	240[a]	524
		n-Pentanol	360	333.5[a]	286	240[a]	—	—	—	527
		Chloroform	362	336.5[a]	288	—	—	—	—	522
		Aqueous surfactant above the CMC	360	334	(308)	(295)	240[a]	—	—	524
Hexadecyltrimethylammonium bromide	6.8	Water	335	326[a]	307[a]	(296)	280[a]	240[a]	—	522
		Ethanol	333	(322)	307	(292)	280	240[a]	—	522
		n-Pentanol	334	325[a]	307[a]	(293)	282	240[a]	—	526
		Chloroform	336	327[a]	307[a]	(294)	283	—	—	526.5
		Aqueous surfactant above the CMC	333	325[a]	(307)	(293)	280[a]	240[a]	—	527
Hexadecyltrimethylammonium bromide	12.8	Water	360[a]	335	327[a]	307[a]	(295)	280[a]	240[a]	522
		Ethanol	370[a]	333	325[a]	307	(294)	280	240[a]	522
		n-Pentanol	358	335	(322)	(305)	(295)	283	240[a]	524
		Chloroform	360[a]	337	(322)	(307)	(295)	286	—	524
		Aqueous surfactant above the CMC	366[a]	333	327[a]	307[a]	(295)	277.5[a]	240[a]	524
Tetradecyltrimethylammonium bromide	6.8	Water	335	328[a]	(308)	(290)	(280)	240[a]	—	522
		Ethanol	332.5	324[a]	305[a]	(293)	280	240[a]	—	522
		n-Pentanol	333	325[a]	307[a]	(293)	280	240[a]	—	523
		Chloroform	336	325[a]	307[a]	(294)	282	—	—	525
		Aqueous surfactant above the CMC	333	324[a]	307[a]	(292)	276[a]	240[a]	—	524.5
Dodecyltrimethylammonium bromide	6.8	Water	335[a]	(295)	240[a]	—[c]	—	—	—	522
		Ethanol	333	325[a]	306.5	(293)	281	240[a]	—	522
		n-Pentanol	335	324	307[a]	(294)	283	240[a]	—	525
		Chloroform	336	327[a]	308[a]	(295)	283	—	—	527
		Aqueous surfactant above the CMC	334	327[a]	(307)	(293)	(282)	240[a]	—	527
Cetrimide	6.8	Water	335[a]	(295)	—[c]	—	—	—	—	522
		Ethanol	333	324.5[a]	307	(292)	280	240[a]	—	522
		n-Pentanol	334	325[a]	(310)	(293)	282	240[a]	—	525
		Chloroform	337	327.5[a]	(312)	(295)	283	—	—	528
		Aqueous surfactant above the CMC	333	325[a]	307	(292)	279[a]	(245)	—	524

[a] An inflection. [b] Numbers in parentheses represent a shoulder. [c] Slow coacervation causing "flattening" of peaks (see text).

Table VIII, and the effect of sodium chloride is detailed in Table IX. In 0.1 *N* NaOH at pH 12.0, flocculation or coacervation did not occur.

When dye–surfactant solutions containing a slight excess of surfactant for compatibility were heated, the dye–surfactant complex precipitated as a coacervate (see *Microscopic Investigation*). The coacervation temperature for these systems, with surfactant above the CMC and a dye concentration of 1.5 mmoles/l. can be seen in Fig. 8. Table X gives the data for surfactants below the CMC and a dye concentration of 0.15 mmole/l. Curves similar to those of Fig. 8 are obtained when these data are graphed. All systems were reversible with respect to temperature; *i.e.*, when solutions cooled after heating, the coacervate disappeared. The effect of dye concentration on these curves can be seen from Figs. 9–11, where data are plotted for dodecyltrimethylammonium bromide– and hexadecyltrimethylammonium bromide–dye solutions. At pH values above about 9.5, no coacervation was observed. The effect of different salts on the temperature of coacervation is presented graphically in Fig. 12*a* for one clear uncoacervated dye–cetrimide solution (1.5 mmoles/l. dye and 7.0 mmoles/l. cetrimide). Figure 12*b* indicates that the concentration of cetrimide in the uncoacervated dye–surfactant–water system influences the coacervation phenomenon in NaCl solution. Cetrimide concentrations used were 6.5, 7.0, and 7.5 mmoles/l., with a constant dye concentration of 1.5 mmoles/l.

Figure 13 shows the effect of surfactant concentration (C_S, millimoles per liter) of three homologs on the specific viscosity (η_{sp}) of aqueous dye–surfactant solutions above and below the CMC; η_{sp} is defined as $(\eta_S - \eta_O)/\eta_O$, where η_S and η_O are the viscosities of the solution and solvent, respectively. The solvent for data represented in Fig. 13 was considered to be the dye solution. The dotted portion of the curves represents the incompatible region as defined by the appearance of turbidity in the systems. The viscosities of some coacervated systems were determined, and it can be seen that the

Table VII—Concentrations at Points of Inflection or Minima in Surface Tension and Light-Scattering Curves for Amaranth–Alkyltrimethylammonium Bromide Complexes

Alkyltrimethylammonium Bromide	Concentration, g. ml.$^{-1}$ × 10^{-5} — Surface Tension — 3:1 Surfactant–Dye Complex	Surface Tension — 4:1 Surfactant–Dye Complex	Light Scattering — 3:1 Surfactant–Dye Complex	Light Scattering — 4:1 Surfactant–Dye Complex
Dodecyl-	10.0	—	—	—
Tetradecyl-	1.7	—	—	—
Hexadecyl-	3.0	3.0	4.0	5.0–6.0
Octadecyl-	1.0	1.5	1.5–2.0	1.5

Table VIII—Effect of Temperature on the Minimum Ratio of Cetrimide to Dye for Compatibility (Dye Concentration = 1 mmole/l.)

Temperature	Ratio of Surfactant to Dye
13.5°	4.67:1
23.0°	4.84:1
40.0°	5.08:1
57.0°	5.62:1
76.0°	5.84:1

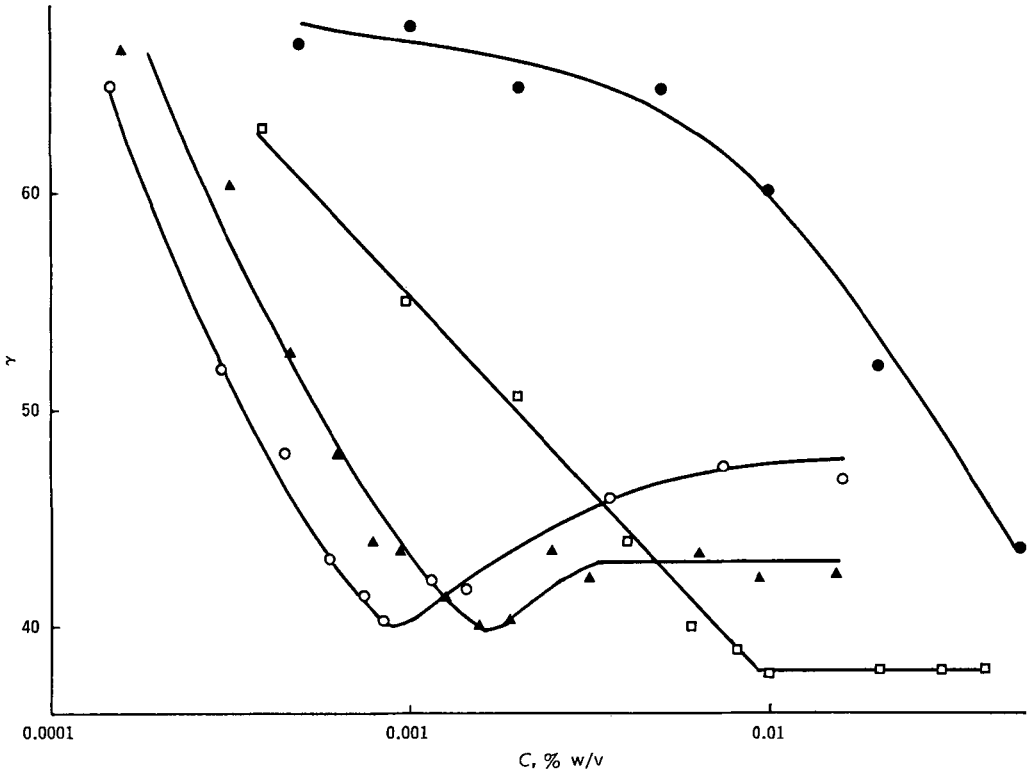

Figure 6—*Plots of surface tension* (γ, *dyne cm.*$^{-1}$) versus *concentration of dye-surfactant complex or dodecyltrimethylammonium bromide* (C, % *w/v*) *at 25°. Key:* □, *dodecyltrimethylammonium bromide-dye (3:1);* ○, *octadecyltrimethylammonium bromide-dye (3:1);* ▲, *octadecyltrimethylammonium bromide-dye (4:1); and* ●, *dodecyltrimethylammonium bromide only.*

specific viscosities were reduced to almost the value for dye solution alone. Viscosities of aqueous dye solutions alone are as follows: 0.15 mmole/l., 0.8924 cps.; and 1.5 mmoles/l., 0.9009 cps. Viscosities of dye solutions at pH 12.0 (0.1 *N* NaOH) are: 0.15 mmole/l., 0.9718 cps.; and 1.5 mmoles/l., 0.9720 cps.

Figure 14 shows viscosity data for dye and surfactant in 0.1 *N* NaOH at pH 12.0. The more viscous solutions, especially hexadecyltrimethylammonium bromide-dye solutions, gave decreasing flow times when passed repeatedly through the capillary viscometer, which indicated that the solutions were non-Newtonian. For these solutions the data represent apparent specific viscosities derived from the initial flow time recorded.

Figure 15 indicates that a similar effect to that in Fig. 13 is obtained, above and below the CMC, when the concentration of dye is varied in aqueous solutions of constant cetrimide concentration. Here, η_O is taken as the viscosity of the cetrimide solution.

Figures 16–18 show plots of the Rayleigh ratio at 90° (R_{90}) *versus* concentration (*C*) and of the dissymmetry (*Z*) *versus* concentration (*C*) for aqueous solutions of octadecyltrimethylammonium bromide-dye crystalline complexes (4:1 and 3:1) and hexadecyltrimethylammonium bromide-dye crystalline complexes (4:1 and 3:1). Figures 19 and 20 illustrate how the coacervation of the system at various concentrations in aqueous solution proceeds with time, as shown by the increase in turbidity (τ). The turbidity of the octadecyltrimethylammonium bromide-dye complex (4:1) did not increase over 2 hr., suggesting that the rate of coacervation for this complex is slow.

The microscopic examination of the turbid solutions encountered proved to be valuable. Dilute aqueous solutions of dye and surfactant when mixed produced perfectly spherical oily droplets (Fig. 21). At higher concentrations, floccules formed which, on closer examination, were found to consist of aggregates of very small oily droplets. Eventually, these floccules disintegrated into oily droplets. This phenomenon was accelerated by heating to about 35° on the Kofler hot-stage when much larger droplets formed. Some droplets coalesced. As the droplets cooled, inside some of them there separated out fresh equilibrium liquid in the form of fine droplets. This process has been called *vacuolation* (27). These changes are shown in the photomicrographs of Fig. 22. The number

Table IX—Effect of Sodium Chloride on the Minimum Ratio of Cetrimide to Dye for Compatibility at 22°

Concentration of Dye in Final Solution, mmoles/l.	Concentration of NaCl, mmoles/l.	Ratio of Surfactant to Dye
1.0	—	4.12:1
	50	4.22:1
	100	3.87:1
	150	3.75:1
	200	3.55:1
2.0	—	4.01:1
	50	3.87:1
	100	3.71:1
	150	3.63:1
	200	3.45:1

Table X—Coacervation Temperatures for Aqueous Dye Solutions of Alkyltrimethylammonium Bromides below the CMC[a]

Alkyltrimethylammonium Bromide							
—Dodecyl—		—Cetrimide—		—Tetradecyl—		—Hexadecyl—	
C_S	Temperature	C_S	Temperature	C_S	Temperature	C_S	Temperature
1.95	28°	0.91	30°	0.62	36°	0.49	52°
2.27	34°	1.19	41°	0.90	40°	0.55	58°
2.59	38.5°	1.49	48°	1.04	43.5°	0.60	66°
2.91	44°	1.79	64°	1.13	45.5°	0.66	73°
3.24	59.5°	2.08	85°	1.19	46.5°	0.69	85°
3.56	74°	—	—	1.34	54°	—	—
3.70	84°	—	—	1.49	69°	—	—
—	—	—	—	1.64	83°	—	—

[a] Concentration of dye is 0.1445 mmole/l. C_S represents concentration of surfactant in millimoles per liter.

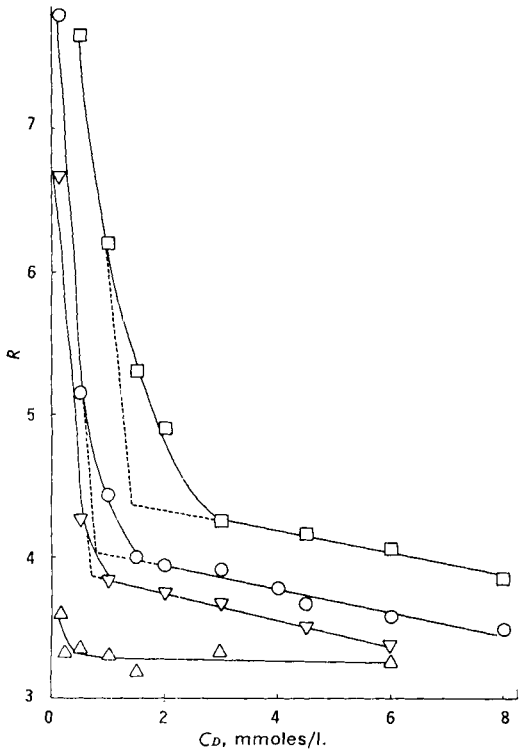

Figure 7—*Phase diagram showing the minimum ratio* (R) *of surfactant to dye for compatibility in aqueous solutions at different concentrations of dye* (C_D, *millimoles per liter*) *at ~22°. Key:* □, *dodecyltrimethylammonium bromide;* ○, *cetrimide;* ▽, *tetradecyltrimethylammonium bromide; and* △, *hexadecyltrimethylammonium bromide.*

of vacuoles formed depended on the size of the coacervate drop (the larger the drop, the more vacuoles formed) and the rate of heating and cooling. After about 1 hr., floccules again reformed.

When one of the uncoacervated dye–surfactant systems used in the heating experiments was heated on the Kofler hot-stage, there was a distinct temperature at which coacervate droplets formed. This temperature corresponded to the appearance of turbidity in the heating experiments. The droplets dissolved when cooled below this temperature.

A microscopic examination of turbid systems produced by dilute aqueous solutions of crystalline dye–surfactant complexes used for light-scattering and surface tension experiments showed that this turbidity was also due to the presence of coacervate droplets.

When one drop of aqueous surfactant solution and one drop of aqueous dye solution were placed close together on a microscope

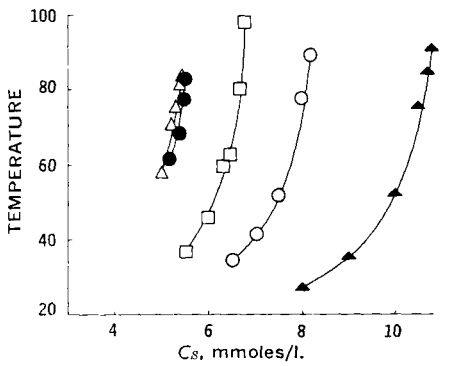

Figure 8—*Temperature of coacervation of dye–surfactant complexes in aqueous solutions of dye and surfactant above the CMC. Dye concentration is 1.5 mmoles/l.; surfactant concentration is* C_S, *millimoles per liter. Key:* ▲, *dodecyltrimethylammonium bromide;* ○, *cetrimide;* □, *tetradecyltrimethylammonium bromide;* △, *hexadecyltrimethylammonium bromide; and* ●, *octadecyltrimethylammonium bromide.*

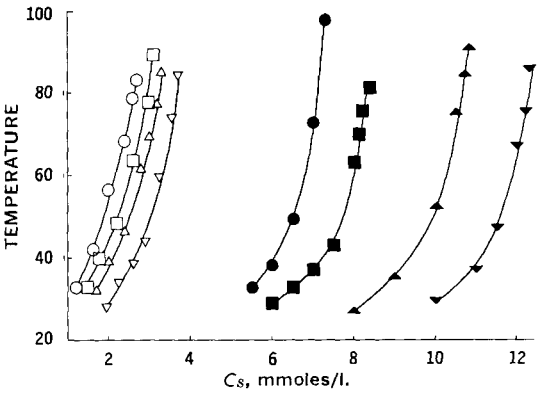

Figure 9—*Graph showing the effect of amaranth concentration on the coacervation temperature of dodecyltrimethylammonium bromide–dye complexes, from aqueous solutions of dye and dodecyltrimethylammonium bromide (concentration* C_S, *millimoles per liter). Open symbols represent curves below the CMC; closed symbols represent curves above the CMC. Concentrations of amaranth (millimoles per liter) are:* ○, *0.05;* □, *0.075;* △, *0.10;* ▽, *0.15;* ●, *0.75;* ■, *1.00;* ▲, *1.50; and* ▼, *2.00.*

slide and allowed to mix slowly by placing a coverslip over both drops, the formation of coacervate droplets at the interface was observed. Figure 23 contains photomicrographs showing the formation of such coacervate droplets.

Droplets examined in an electric field exhibited three effects associated with coacervation (27): (*a*) electrophoresis, (*b*) deformation, and (*c*) disintegration. The electrophoretic behavior of small coacervate droplets formed by mixing dilute aqueous solutions of dye and surfactant in suitable quantities depended on the ratio of surfactant to dye present. At a ratio of 3:1 (expected to be the uncharged complex) droplets focused on in the stationary layer moved very slowly toward the positive electrode, indicating a small negative charge. Compatibility studies, however, showed that in aqueous solution the reversal of charge point does not always coincide with the equivalence point. Coacervate droplets prepared in a solution containing excess dye were negatively charged (definite movement toward the positive electrode), and those prepared in a solution containing excess surfactant possessed a net positive charge (definite movement toward the negative electrode).

The deformation and disintegration phenomena of the coacervate and the behavior of the vacuoles could be observed in large drops. These were formed in the microelectrophoresis cell by heating the small droplets in the cell to about 35°. Larger drops, denser than the surrounding equilibrium liquid, settled on the lower surface of the cell. The drops exhibited deformation in an electric field (Fig. 24), although the rate of this deformation was slow, possibly because of the high viscosity of the coacervate. The degree of deformation was dependent on the original diameter of the drops; small drops deformed less readily than large drops.

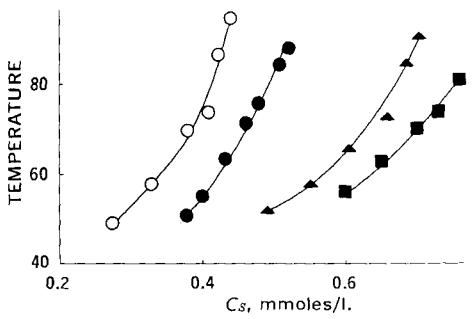

Figure 10—*Graph showing the effect of amaranth concentration on the coacervation temperature of hexadecyltrimethylammonium bromide–dye complexes in aqueous solutions of dye and hexadecyltrimethylammonium bromide below the CMC (concentration* C_S, *millimoles per liter). Concentrations of amaranth (millimoles per liter) are:* ○, *0.072;* ●, *0.100;* ▲, *0.1445; and* ■, *0.175.*

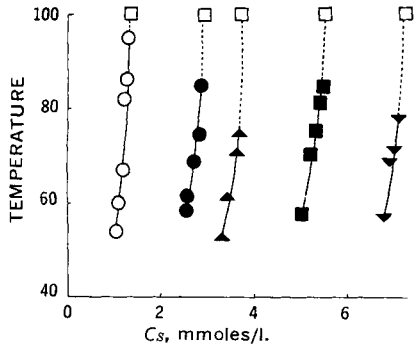

Figure 11—*Graph showing the effect of amaranth concentration on the coacervation temperature of hexadecyltrimethylammonium bromide–dye complexes from aqueous solutions of dye and hexadecyltrimethylammonium bromide above the CMC (concentration* C_S, *millimoles per liter). Concentrations of amaranth (millimoles per liter) are:* ○, *0.29;* ●, *0.75;* ▲, *1.00;* ■, *1.50; and* ▼, *2.00.* □ *represents no coacervation at 100°.*

Vacuoles within a large coacervate drop were also affected by an electric field. They were transported in the direction of the cathode in the case of positive coacervate droplets and toward the anode in the case of negative coacervate droplets. When vacuoles arrived at the surface of the coacervate droplet, they protruded and were ejected into the equilibrium liquid into which they disappeared. At the opposite side of the large drop, many new small coacervate droplets formed in the equilibrium liquid a short distance from the original coacervate interface. The photomicrograph of Fig. 25 clearly shows the formation of these new small droplets.

Results for the approximate analysis of a coacervated system showed that the approximate percentage of dye and surfactant retained in the coacervate was 94.2 and 98.3, respectively.

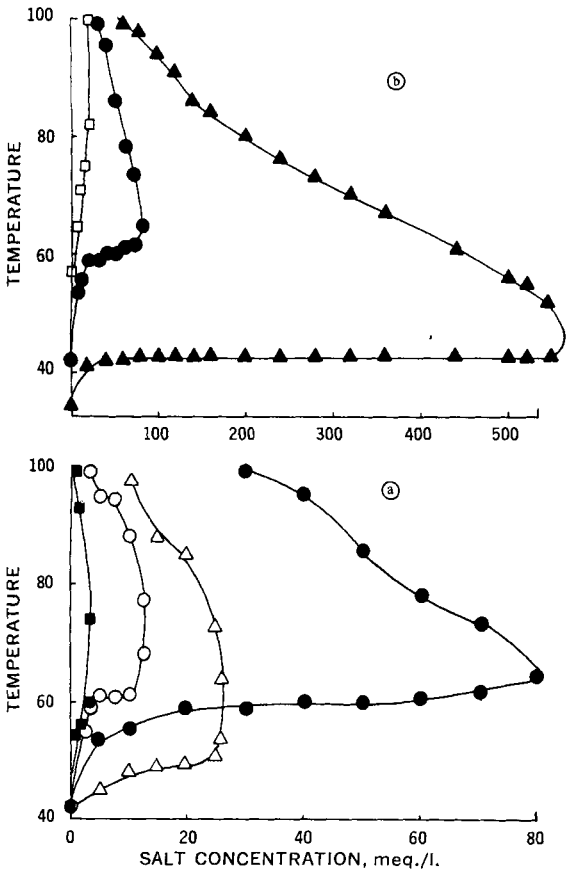

Figure 12—(*a*) *Effect of cation and anion valency of added salt on the temperature of coacervation of an aqueous solution of cetrimide (7.0 mmoles/l.) and dye (1.5 mmoles/l.). Key:* ●, *NaCl;* ○, Na_2SO_4; ■, *sodium citrate; and* △, $CaCl_2$. (*b*) *Effect of NaCl concentration on the temperature of coacervation of some aqueous solutions of amaranth and cetrimide. Key:* ▲, *6.5 mmoles/l. cetrimide;* ●, *7.0 mmoles/l. cetrimide; and* □, *7.5 mmoles/l. cetrimide. Concentration of dye is 1.5 mmoles/l.*

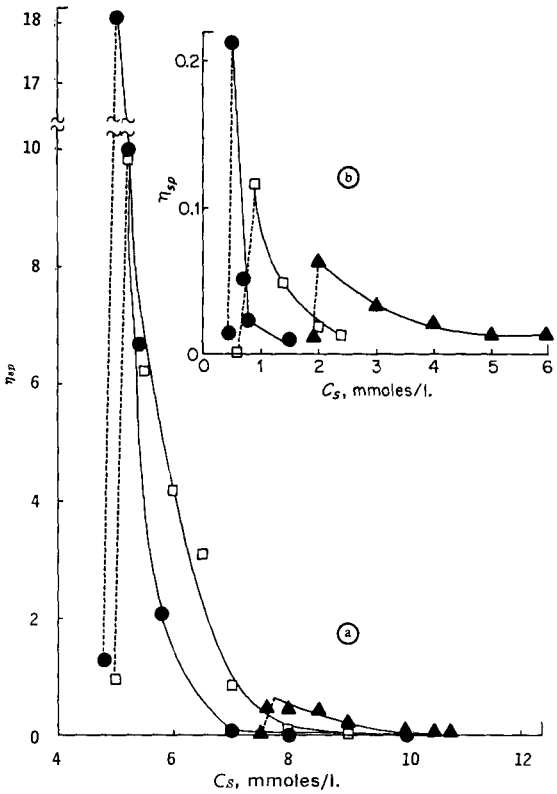

Figure 13—*Effect of surfactant concentration* (C_S, *millimoles per liter) and alkyl chain length on the specific viscosity* (η_{sp}) *of aqueous dye solutions: (a) surfactant above the CMC and 1.5 mmole/l. dye, and (b) surfactant below the CMC and 0.15 mmole/l. dye. Key:* ▲, *dodecyltrimethylammonium bromide;* □, *tetradecyltrimethylammonium bromide; and* ●, *hexadecyltrimethylammonium bromide. Dotted regions represent coacervated systems.*

DISCUSSION

The experiments considered in this paper led to the idea that interaction is a coacervation phenomenon; for clarity and ease of discussion, the procedure that occurred in practice will be reversed and it will be assumed that interaction is due to coacervation and results will be explained with respect to general coacervation theory.

Experimental Results Relating to Stoichiometry and Properties of Dye–Surfactant Complexes—The constancy of the visible spectrum of aqueous amaranth solution from pH 2.6 to 9.0 indicates that the sulfonate groups are completely ionized and the phenolic group is unionized over this range of pH (Fig. 1). Above pH 9.0 the color alters owing to ionization of the phenolic auxochrome. This causes the absorbance to decrease from 0.77 at pH 9.0 to 0.445 at pH 12.0 and the $\lambda_{max.}$ to shift from 522 to 490 nm. Although the percentage OH ionized at any pH can be predicted from the Henderson–Hasselbalch equation, a knowledge of the color change of the dye with pH is desirable before commencing any stability tests. The UV spectrum is a modified naphthalene absorption, the peaks at 277 and 240 nm. being K- or E-bands and the peak at 332 nm. a B-band. All these bands can be ascribed mainly to π–π^* transitions. The B-band corresponds to forbidden transitions and is, therefore, much less intense than the K- or E-bands. The bathochromic shift observed at pH 12.0 is again attributed to dissociation of the phenolic auxochrome, which would be expected to modify the UV spectrum in this manner.

It would be expected that the stoichiometric relationship of a complex formed between monovalent ions of opposite charge would

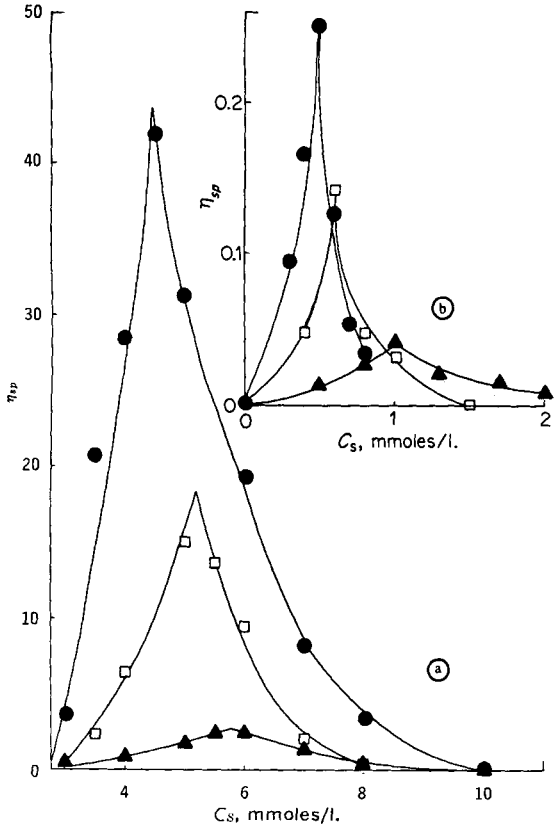

Figure 14—*Effect of surfactant concentration* (C_S, *millimoles per liter*) *and alkyl chain length on the specific viscosity* (η_{sp}) *of 0.1* N *NaOH–dye solutions: (a) surfactant above the CMC and 1.5 mmoles/l. dye, and (b) surfactant below the CMC and 0.15 mmole/l. dye. Key:* ▲, *dodecyltrimethylammonium bromide;* □, *tetradecyltrimethylammonium bromide; and* ●, *hexadecyltrimethylammonium bromide.*

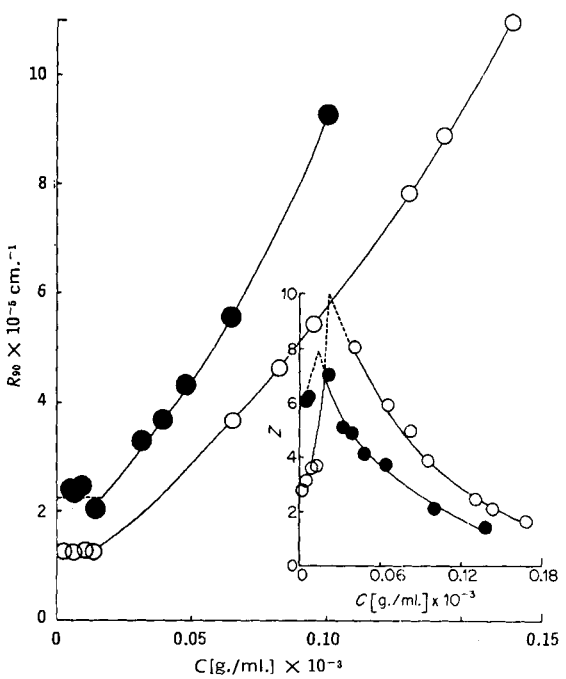

Figure 16—*Plots of the Rayleigh ratio at 90°* (R_{90}) versus *concentration,* C *[g./ml.]* × 10^{-3}, *and dissymmetry* (Z) versus *concentration (inset) for octadecyltrimethylammonium bromide–dye complexes at 25°. Key:* ●, *4:1 complex; and* ○, *3:1 complex. Dotted portions represent an approximate extrapolation.*

be 1:1. Since amaranth has three negatively charged sulfonate groups, any complex formed between itself and the alkyltrimethylammonium bromides is expected to have a 1:3 stoichiometry. Figure 2 indicates that for octadecyltrimethylammonium bromide and hexadecyltrimethylammonium bromide the number of moles of amaranth transferred to the chloroform phase was in all cases equal to a third of the number of moles of octadecyltrimethylammonium bromide or hexadecyltrimethylammonium bromide, thus indicating the expected 1:3 stoichiometry. Plots for tetradecyltrimethylammonium bromide, cetrimide, and dodecyltrimethylammonium bromide deviate from linearity. This indicates that although the formation of the dye–cation complex depends on electrostatic interaction between opposite charges, the efficiency of extraction depends on the chain length of the surfactant. An increase in chain length increases solubility in chloroform. Whereas the drop in extraction efficiency is slight between hexadecyltrimethylammonium bromide- and tetradecyltrimethylammonium bromide–dye complexes, the efficiency is only about one-half for the dodecyltrimethylammonium bromide–dye complex. That the curves do not pass through the origin is attributed to the fact that a small amount of surfactant is transferred to the chloroform phase even in the absence of dye. Further extractions of tetradecyltrimethylammonium bromide–dye solutions also yielded a straight line of gradient one-third. Although complete extraction of dodecyltrimethylammonium bromide- and cetrimide–dye complexes was not attained, it is a reasonable assumption that there is also a 1:3 relationship here. At pH values greater than 11, where the

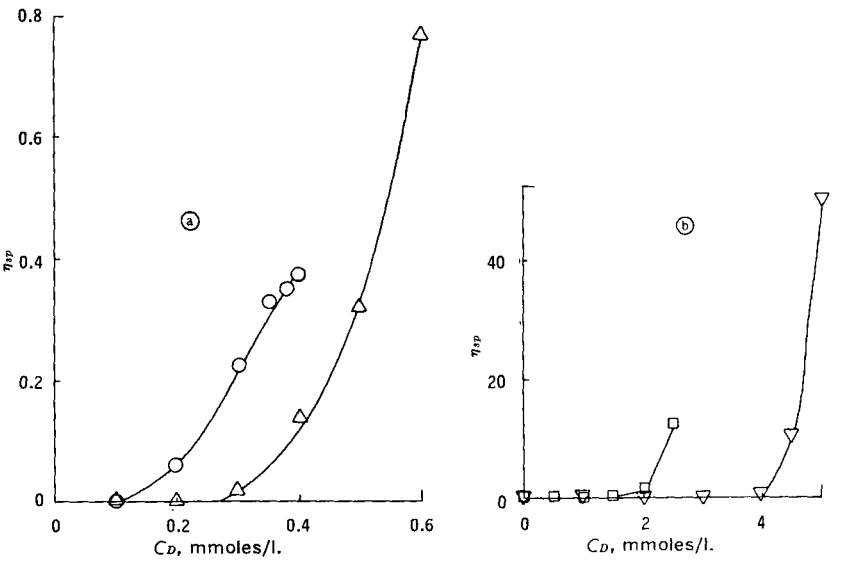

Figure 15—*Effect of dye concentration* (C_D, *millimoles per liter*) *at four different concentrations of cetrimide on the specific viscosity* (η_{sp}) *of surfactant–dye solutions. (a) Concentrations of cetrimide below the CMC:* ○, *2 mmoles/l.; and* △, *3 mmoles/l. (b) Concentrations of cetrimide above the CMC:* □, *10 mmoles/l.; and* ▽, *20 mmoles/l.*

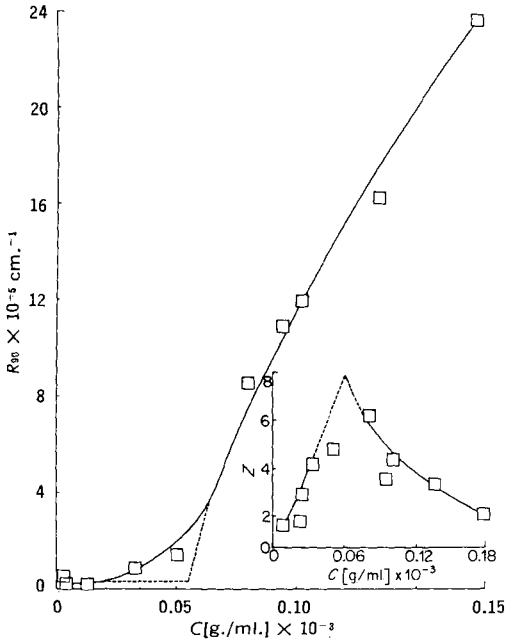

Figure 17—*Plots of the Rayleigh ratio at 90°* (R_{90}) versus *concentration*, C [*g./ml.*] × 10^{-3}, *and dissymmetry* (Z) versus *concentration* (*inset*) *for hexadecyltrimethylammonium bromide–dye* (*4:1*) *complex at 25°*.

phenolic OH of amaranth is completely dissociated, 1 mole of amaranth was transferred for every 4 moles of surfactant, indicating a 1 : 4 relationship. Figure 3 also clearly indicates that the complexes are more easily extracted at lower hydrogen-ion concentrations. The concentrations of alkyltrimethylammonium bromides used were below the CMC (Table III), which excludes the possible interference of surfactant micellar species.

These observations are substantiated (within experimental error) by elemental analysis of the four most easily extractable complexes. Since all the commercial alkyltrimethylammonium bromides contain other homologs as impurities, the expected values for percentage C, H, and N content of each complex were estimated from the analytical results given in Table I, ignoring any possible interaction of the small amounts of parent alkyl bromides with the dye which were shown not to interfere (*28*). It is also assumed that the dye interacts with the commercial surfactants so as to give complexes in which the different cationic homologs are present in the same ratios as in the starting material; *i.e.*, there is no *preferred* reaction based on chain length of surfactant. In view of these assumptions and approximations, the agreement between estimated and found percentages is acceptable.

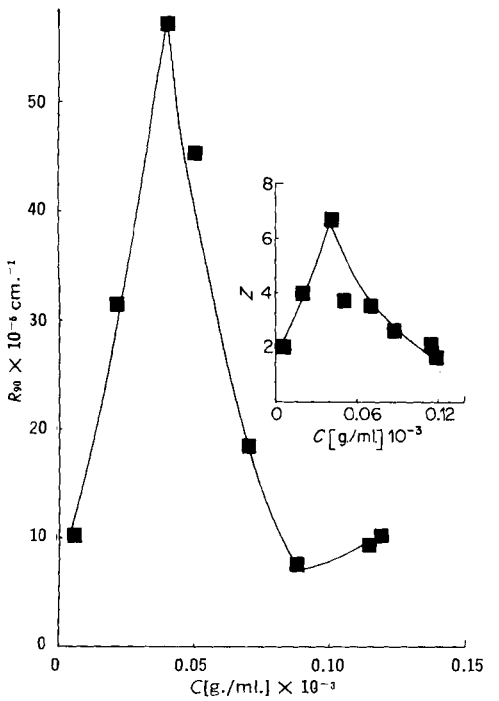

Figure 18—*Plots of the Rayleigh ratio at 90°* (R_{90}) versus *concentration*, C [*g./ml.*] × 10^{-3}, *and dissymmetry* (Z) versus *concentration* (*inset*) *for hexadecyltrimethylammonium bromide–dye* (*3:1*) *complex at 25°*.

IR spectra indicate no major structural changes in the dye or surfactant on interaction. This is to be expected if interaction is by means of electrostatic bonding only.

The microscopic examination between crossed polars shows that crystals obtained at both neutral and alkaline pH possess the optical properties of a uniaxial crystal. The crystallography of the complexes was not investigated further. The melting points of the tetradecyltrimethylammonium bromide–, cetrimide–, and dodecyltrimethylammonium bromide–dye complexes were similar, a result not unexpected considering the composition of the parent homologs (Table I). Complexes of the higher homologs have higher melting points.

Riegelman *et al.* (23) and Riegelman (29) showed that the UV spectrum of a solubilizate can be used to determine its mode of solubilization in micellar solution. The four different modes postulated by these workers are: (*a*) inclusion into the hydrocarbon interior of the micelles, (*b*) deep penetration of the palisade layer, (*c*) short penetration of the palisade layer, and (*d*) adsorption onto the surface of the micelle. Changes in the UV spectrum due to variations of pH and molecular interactions are usually large. Small changes may be due to the environment affecting either the polarizability of the valence electrons or the permanent or induced dipoles. Relative to the absorption bands of the complexes in water, their spectra in solvents of decreasing dielectric constant illustrate the effect of changes in polarizability of the electrons. By taking peaks and inflections of the spectrum in ethanol as comparison standards, it can be seen from Table VI that the absorption maxima are shifted toward longer wavelengths in chloroform, and more fine structure is noted. The spectra of both the neutral and alkaline complexes in aqueous surfactant solution above the CMC are very similar to their spectra in ethanol; *i.e.*, the complexes behave as if they are in an environment similar to that of ethanol. From these observations it is not possible to locate exactly the position of the complex in the micelle, but it may be concluded that the complex is certainly not solubilized in the hydrocarbon interior of the micelle but is probably orientated in the palisade layer.

The spectra in water are somewhat anomalous as peaks should be of shorter wavelengths than in ethanol. Aqueous solutions of the cetrimide complex and dodecyltrimethylammonium bromide complex precipitated slowly after only a short period of standing, causing a "flattening" of the spectra. The UV and visible spectra of the cetrimide complex were found to change with time. After 1 hr., the inflection at 335 nm. had moved to 337 nm. and the peak in the visible region had moved from 522 to 528 nm. These changes are associated with the formation of a coacervate which develops on standing.

Coacervation in Dye–Surfactant Systems—The formation of oily droplets in a colloidal system, to which a second colloidal species of opposite charge has been added, was termed complex coacervation by Bungenberg de Jong and Kruyt (30, 31). They regarded the coacervate state as an "arrested precipitation" of the colloidal species, and they showed that it was quite stable but also reversible; *i.e.*, if the conditions that initiated coacervation were changed even slightly, the solution could revert to the homogeneous state or flocculate or precipitate. Coacervate droplets are rich in colloid, but the remaining liquid from which they separate—the equilibrium liquid—is poor in colloid. The simple analysis of a coacervated system of amaranth and alkyltrimethylammonium bromide showed that this was so for systems in this study. The oldest observations in this field were of the combination of basic proteins with nucleic acids (32) to form precipitates with glutinous properties or oil-like drops (33). Complex coacervation in gum arabic–gelatin and sodium arabinate–hexol nitrate systems were examined in detail by Bungenberg de Jong and Dekker (34).

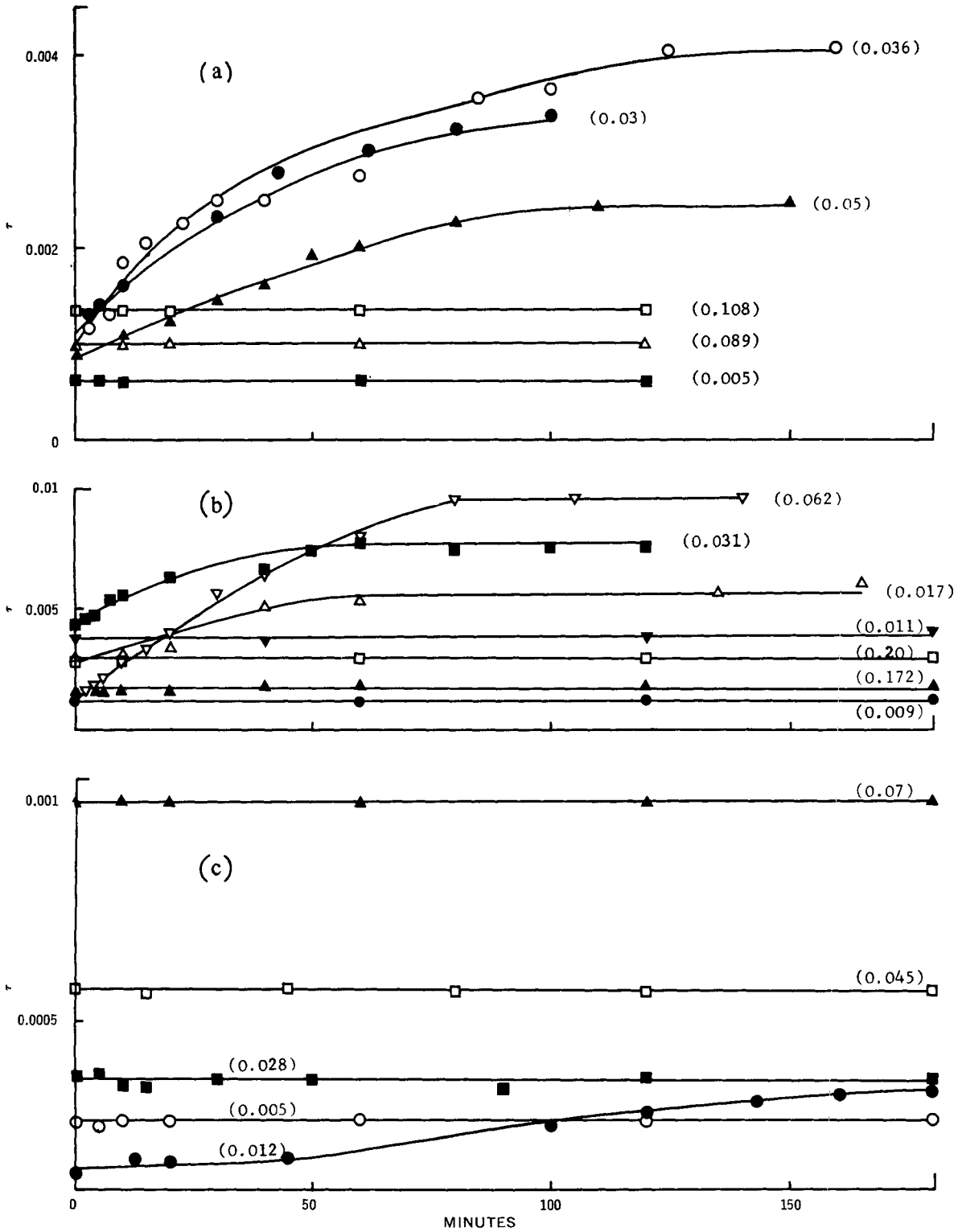

Figure 19—*Plots of turbidity* (τ) versus *time (minutes) at 25° for: (a) hexadecyltrimethylammonium bromide–dye (4:1) complex, (b) hexadecyltrimethylammonium bromide–dye (3:1) complex, and (c) octadecyltrimethylammonium bromide–dye (3:1) complex at different concentrations (figures in parentheses, g. ml.*$^{-1} \times 10^{-3}$).

The microscopic examination clearly showed that in amaranth–alkyltrimethylammonium bromide–water systems, according to the conditions, a coacervate or flocculate was formed, the latter consisting of coacervate droplets linked together. Similar phenomena were observed for the gelatin–phosphatide (an association colloid) system, which under certain conditions formed floccules consisting of small coacervate droplets (35). It was suggested that flocculation rather than coacervation occurs by rapid considerable desolvation of the particles. This causes the coacervate to become so extremely viscous due to the appreciably smaller thickness of the hydration layer that fusion of the droplets into larger ones is retarded (27).

The behavior of the coacervate droplets in an a.c. electric field was typical of such systems (27). The deformation of the droplets to an ellipsoidal shape is called the Büchner effect (36). This depends on the difference in conductivity between coacervate and equilibrium liquid. The coacervate conductivity is lower than that

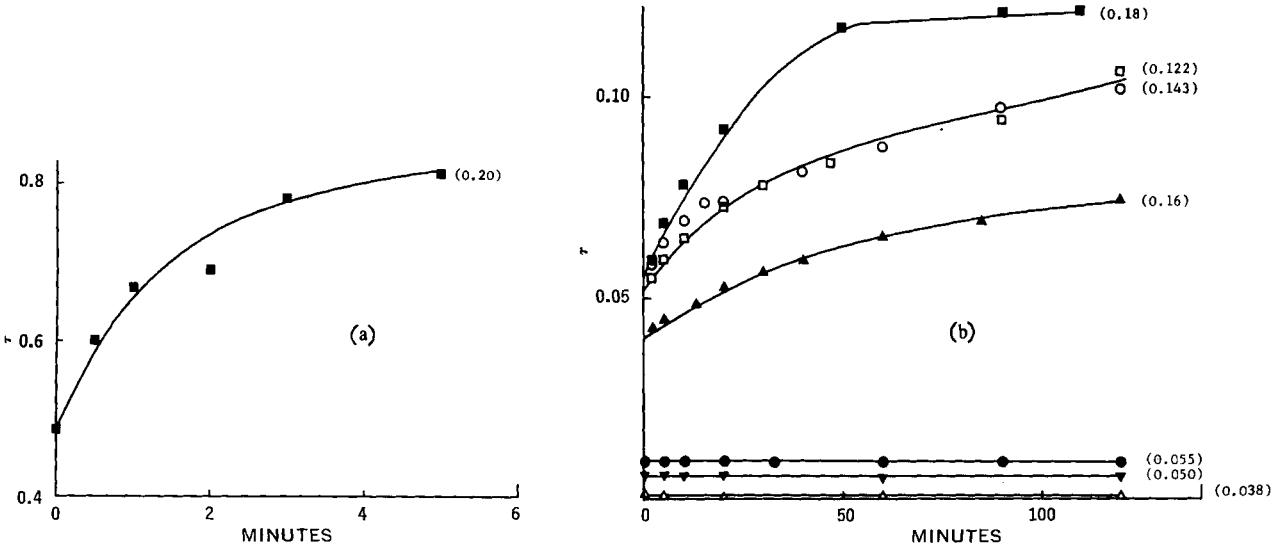

Figure 20—*Plots of turbidity* (τ) versus *time (minutes) at 25° for: (a) dodecyltrimethylammonium bromide–dye (3:1) complex, and (b) tetradecyltrimethylammonium bromide–dye (3:1) complex at different concentrations (figures in parentheses, g. ml.*$^{-1} \times 10^{-3}$).

of the equilibrium liquid in these studies, as shown by the way the flattening takes place perpendicular to the lines of force. The disintegration phenomenon and the formation of a "crown" of small coacervate droplets in the equilibrium liquid on one side of the large drop may be explained by the theory of Bungenberg de Jong (27). The two colloid components of the complex coacervate are not rigidly bound to each other and, thus, they are displaceable in an electric field. The surfactant cations move in the direction of the cathode and the dye anions in the direction of the anode. If the system contains excess surfactant, cations attempting to leave the large droplet on the cathode side do not form new droplets; however, dye anions leaving the opposite side encounter fresh surfactant in the equilibrium liquid and are able to form new coacervate droplets. This explains why positively charged coacervate droplets (*i.e.*, those prepared in excess surfactant) form a "crown" of coacervate droplets in the equilibrium liquid exclusively on the anode side.

The surface tension curves for the dye-surfactant complexes (Figs. 5 and 6) all exhibit either a "leveling off" phenomenon or a minimum consistent with a typical CMC curve for surfactants. However, in view of the microscopic examination of some of the solutions which became turbid on standing, it is unlikely that all these surface tension results were determined in stable solutions; some probably were made in coacervating systems. It is, therefore, probable that the breaks and minima in the surface tension curves correspond to the coacervation limits of the complexes rather than to true CMC's. It has been shown that some azo dyes (37, 38) form micelles at high concentrations, but the surface tension curve for the dye solution alone (Fig. 5) shows that dye micelles are not present at the low concentrations used in this work. These coacervation limits were confirmed by light-scattering data where dissymmetry measurements clearly showed the formation of coacervate at a particular concentration of the complex in water. Concentrations obtained from both methods were of the same order (Table VII). Close agreement was not expected since measurements had to be made on relatively unstable systems. The change of turbidity with time of some of these solutions confirmed this instability. When these graphs (Figs. 19 and 20) are compared with the plots of R_{90} *versus* concentration of complex (*C*) (Figs. 16–18), it can again be seen that coacervation commences near the break in the R_{90} *versus C* curves. Since dilute aqueous solutions of the complexes are unstable, it is somewhat surprising that R_{90} values leveled off to an almost constant value. For the hexadecyltrimethylammonium bromide–dye complex (3:1), a maximum was obtained in the R_{90} *versus C* plot (Fig. 18) because turbidity occurred before measurements could be completed. This maximum, together with the maxima of the dissymmetry *versus* concentration curves (insets of Figs. 16–18), suggests that the size of the coacervate reaches a maximum value after which it becomes more dispersed on further dilution.

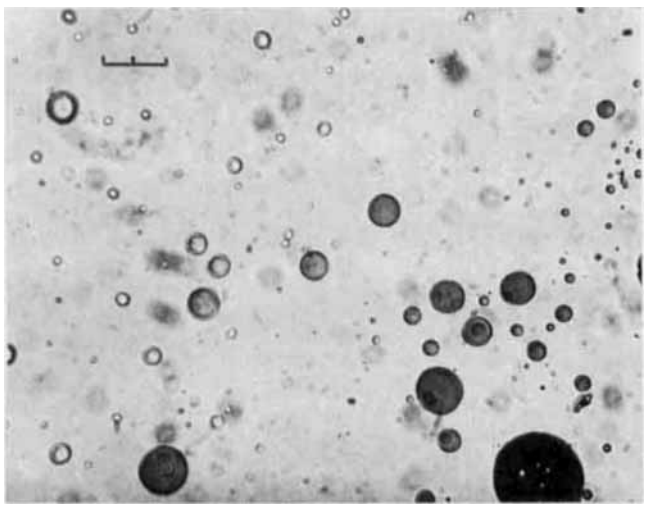

Figure 21—*Formation of coacervate droplets by mixing aqueous solutions of amaranth and alkyltrimethylammonium bromide; 1 division = 20 μ.*

Figure 7 shows that for a given amount of quaternary ammonium salt, the amount of aqueous amaranth solution that can be added before coacervation occurs depends on: (*a*) the alkyl chain length of the surfactant, and (*b*) the concentration of dye. Each curve of Fig. 7 shows a discontinuity at a particular ratio of surfactant to dye which was interpreted as the concentration of surfactant at which micelles form. The curves are similar in shape to surface tension plots for CMC determinations, and the break point is similarly taken as the point of intersection of the two straight-line portions of the curves. The concentrations of surfactant at these ratios are: cetrimide, 3.2 mmoles/l.; dodecyltrimethylammonium bromide, 6.3 mmoles/l.; tetradecyltrimethylammonium bromide, 2.7 mmoles/l.; and hexadecyltrimethylammonium bromide, 0.99 mmole/l. These values are in reasonable agreement with CMC values in Table III when allowances are made for the accuracy of this experiment and for the possible change in CMC due to the presence of the dye. It has been shown that alkyltrimethylammonium bromides form a 3:1 (surfactant-to-dye) extractable complex, and an explanation is needed of the higher ratios (especially below the CMC) of surfactant to dye required for compatibility.

It was expected from the stoichiometry experiments that in aqueous solution an amount of surfactant ions, equivalent to three times the amount of ionized dye groups present, would be sufficient to neutralize the negative charges of the dye. However, the phase study titrations suggest that to reach the reversal of charge point, a quantity of surfactant cations somewhat greater than the

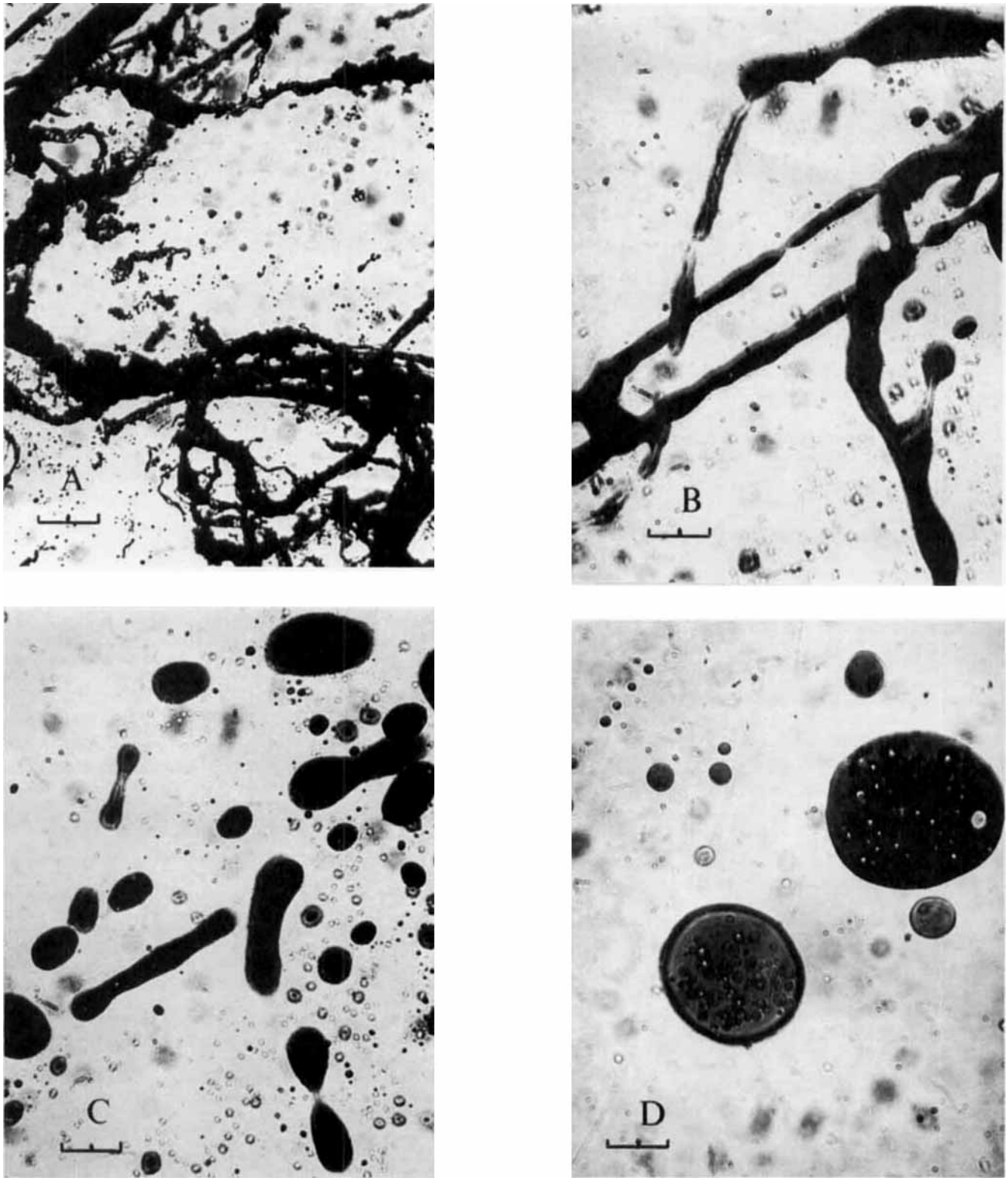

Figure 22—*A shows the formation of floccules on mixing concentrated aqueous solutions of amaranth and alkyltrimethylammonium bromide at room temperature. B, C, and D show the changes observed when the floccules are heated to 35°. D shows vacuoles in coacervate droplets. One division = 20 μ.*

equivalent amount must be bound to the dye anion. This is explained by the fact that the reversal of charge point relates to the electrical properties of the phase boundary of the coacervate droplets. The reversal of charge point was assumed to be indicated by the appearance of a coacervate when an aqueous solution of dye was added to an aqueous solution of surfactant or the disappearance of coacervate when excess surfactant solution was added to dye solution; both methods gave the same ratio of surfactant to dye. The interaction between dye and surfactant may be represented by the equation: $Na_3D + 3RBr \rightarrow 3NaBr + R_3D$, where D and R represent the dye anion and surfactant cation, respectively. This formula is oversimplified, since a coacervate contains a considerable and variable amount of water and various amounts of complex ions (D and R), depending on whether the coacervate is pre-

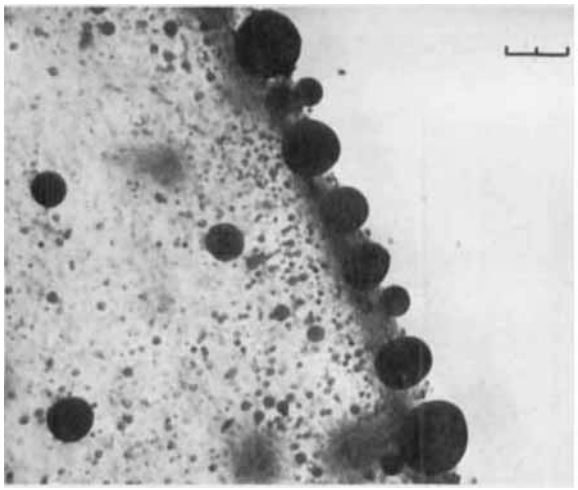

Figure 23—*Formation of coacervate droplets at the interface of aqueous dye and surfactant solutions; 1 division = 20 μ.*

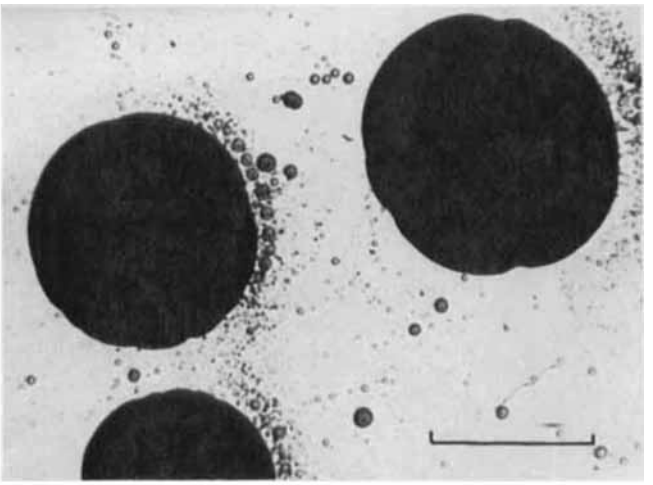

Figure 25—*Disintegration phenomenon in an electric field; 1 division = 100 μ.*

pared in the presence of excess dye or excess surfactant. The coacervate may then be represented as follows:

in excess surfactant	$(R_3D + RBr + H_2O)^+$
in excess dye	$(R_3D + Na_3D + H_2O)^-$

where the net charge arises from adsorption of excess ions and a contribution due to surface dissociation. Thus, at only a definite relative proportion of dye and surfactant in the total system will the coacervate contain equivalent amounts of dye and surfactant ions, *i.e.*, $(R_3D + H_2O)^0$.

It is proposed that this "neutral" coacervate still carries a negative charge at the droplet surface caused by the dissociation of the complex at the surface. A similar proposal was made previously (27, 39) for the sodium arabinate–hexol nitrate system, where the neutral coacervate was shown by electrophoresis to possess a small negative charge. The fact that the amaranth–alkyltrimethylammonium bromide coacervates, prepared in aqueous solution which contained surfactant and dye in the ratio 3:1, moved very slowly to the positive electrode supports this proposal. This new neutral coacervate may then be formulated as $(R_3D + H_2O) - D^{-3}R^+$. The reversal of charge point then becomes the point at which the negative charge of the neutral coacervate is just compensated for by the positive charge of surfactant adsorbed at the surface.

As the surfactant chain length and dye concentration increase, the concentration of surfactant required for charge reversal decreases (Fig. 7). This may be explained using the arguments of Voorn (40), who showed that increase in chain length favors coacervation. Bungenberg de Jong (27) suggested that the tendency of the organic ions to escape from the aqueous medium is important in this phenomenon. In a homologous series, this tendency increases with hydrocarbon chain length. It was assumed that the greater this "escaping tendency," the more easy will be the fixation of the organic ions onto the ionized group; *i.e.*, the reversal of charge concentration will decrease with increasing hydrocarbon chain length.

When micelles are present in the system, the ratio of surfactant to dye for reversal of charge levels off.

At a constant concentration of dye, the concentration of surfactant required to reach the reversal of charge point increases with an increase in temperature (Table VIII). This may be explained on thermodynamic arguments.

Table IX clearly shows that the electrolyte suppresses coacervation; the more salt present, the less surfactant is required to produce a homogeneous system. If sufficient salt is added, coacervation is suppressed completely. In the presence of this electrolyte, the charged groups on the interacting species are screened by dense ionic atmospheres formed around each charge. This diminishes their interactions and, consequently, the mutual attraction between the groups.

Four main points emerge from the data relating to the effect of heat on the dye–surfactant solutions: (*a*) for a given alkyltrimethylammonium bromide, the temperature of coacervation of the dye–surfactant complex increases as the concentration of surfactant increases (Fig. 8); (*b*) for a constant temperature, the concentration of surfactant in solution required for coacervation varies according to the alkyl chain length of the surfactant (the shorter the alkyl chain length, the more surfactant is required for coacervation) (Fig. 8) and whether or not surfactant micelles are present (Fig. 9); (*c*) for a given alkyltrimethylammonium bromide, the concentration of surfactant required for coacervation of the complex at one particular temperature depends on the concentration of dye present (the less dye present, the less surfactant is required) (Figs. 9–11); and (*d*) the coacervation behavior for a particular surfactant at any one temperature and dye and surfactant concentration depends markedly on the concentration of added salt and its valency (Fig. 12). These observations are not unexpected since similar conclusions were derived from the phase separation experiments. However, (*a*) and (*d*) require further discussion.

Voorn (40) treated complex coacervation thermodynamically and derived an expression for the change in total free energy, ΔF, on coacervation:

$$\Delta F = \Delta F_{el} + \Delta F_{mix} \qquad \text{(Eq. 1)}$$

or

$$\Delta F = \Delta F_{el} - T\Delta S_{mix} \qquad \text{(Eq. 2)}$$

where F_{el} represents the electrical free energy of interaction (Coulomb interaction), all interactions of a different nature being neglected; F_{mix} is the total free energy of mixing; S_{mix} is the total entropy of mixing; and T is the absolute temperature. F_{el} was evaluated using the Debye-Hückel theory (41), and TS_{mix} was obtained using the lattice model theory of Flory–Huggins (42). Voorn (40) concluded that favorable conditions for complex coacervation were high charge density (more gain in electrical energy) and

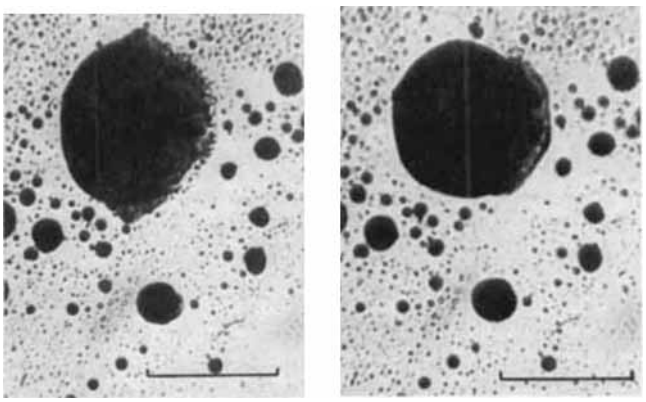

Figure 24—*Deformation phenomenon in an electric field; 1 division = 100 μ.*

great chain length (less loss in entropy). When the temperature increases, the entropy term in Eq. 2 becomes more negative, which favors coacervation. Thus dye–surfactant solutions that are homogeneous at room temperature coacervate at higher temperatures. The more excess surfactant in the system above that required to reach the reversal of charge point, the higher is the temperature required to coacervate the system. This is because the excess surfactant acts as a simple salt and suppresses coacervation.

Little information is available on the effect of temperature on complex coacervation in general, but coacervation with increase in temperature was observed for some polyelectrolyte systems (43, 44).

The suppressive action of an electrolyte on coacervation was already mentioned. It is not surprising that this effect will be stronger the higher the valency of the added ions. The suppression of coacervation shows the following order, which obeys the Schulze–Hardy rule (45, 46): sodium citrate > sodium sulfate > sodium chloride for anions, and calcium chloride > sodium chloride for cations.

The more excess surfactant (above that required to reach the reversal of charge point) in a dye–surfactant–water system, the less salt is required to suppress coacervation at any one temperature. This is because the surfactant itself acts as added salt (Fig. 12). The curves of Fig. 12 indicate that for some surfactant–dye–salt–water systems, the system coacervates on raising the temperature and at a still higher temperature it reverts to a homogeneous solution. Areas enclosed by the curves of Figs. 12 *a* and 12 *b*, therefore, represent coacervated systems and those outside the curves represent homogeneous systems. With reference again to Eq. 2, the initial formation of the coacervate on raising the temperature was already explained. At the temperature of redispersion, the increase in ΔF_{el} overcomes the decrease in the entropy term and $\Delta F > 0$; this is an unfavorable condition for coacervation and a homogeneous solution forms.

Figures 13 and 14 show that the viscosity increases sharply as the ratio of dye to surfactant increases up to the point when the system coacervates. The ratios of surfactant to dye at these maxima agree well with the ratios for compatibility obtained from Fig. 7. This behavior is exhibited by all the surfactants above and below the CMC. Dye solutions which contain short-chain homologs have a smaller maximum viscosity than those which contain long-chain homologs. With reference to Fig. 13, at the viscosity maximum the concentration of surfactant required to reach the reversal of charge point has just been exceeded and the excess surfactant acts as added salt and suppresses the coacervation by screening the charges on the reacting species. With further addition of surfactant, the ζ-potential progressively rises, colloidal particles repel each other, and the solutions become more mobile. In the limit, the viscosities approach those of the dye-free surfactant solutions. Results above and below the CMC indicate that surfactant micelles are not necessary for interaction to occur between the dye and surfactant. Since a short-chain length is unfavorable for coacervation (40, 47) and a smaller interaction product forms, lower specific viscosity maxima are recorded. Similar viscosity phenomena were reported by Wan (48–50) on the interaction of salicylates, salicylic acid, and benzoic acids with cationic surfactants and by Frank *et al.* (51) on the interaction of polyvinylpyrrolidone with some azo dyes. However, a coacervation phenomenon was not reported for these systems. Figure 15, for cetrimide–dye solutions, shows that the same effect occurs if surfactant concentration remains constant and the concentration of dye increases. Again, a maximum viscosity is observed at a point, in this case just prior to coacervation. Figure 15 also shows that the higher the concentration of the reacting species, the higher the maximum viscosity attainable.

At pH 12.0, no coacervation was observed. The viscosity reached a maximum as the concentration of surfactant increased and then decreased as the surfactant concentration increased still further (Fig. 14). Solutions above the CMC, particularly those of tetradecyltrimethylammonium bromide and hexadecyltrimethylammonium bromide, were non-Newtonian and showed viscoelastic effects. These phenomena were not studied further in detail, but it is possible, by increasing the concentration of reactants, to produce a gel-like material amenable to viscoelastic techniques and to which linear viscoelastic theory may be applied. It is possible that the NaOH suppresses coacervation in this system or that the extremely viscous nature of the system restricts the movement of the surfactant and dye molecules and this inhibits interaction. The maxima of these curves do not correspond to the same surfactant-to-dye ratios obtained from the maxima of Fig. 13. At pH 12.0 the hydroxyl group of the amaranth is fully ionized, thus altering the effective equivalent weight. Bungenberg de Jong and Dekker (34) showed that apparent equivalent weights play an important part in complex coacervation. They observed shifts in the ratio of gelatin to gum arabic required for coacervation as the pH varied.

CONCLUSIONS

Few and Ottewill's method (22) for determining the stoichiometry of dye–surfactant complexes was applied to the amaranth quaternary system. Crystalline complexes were extracted with chloroform from aqueous solutions of dye and surfactant and shown to have a stoichiometry of 3:1 (surfactant–dye) at pH 4.8–10.1 and 4:1 at pH 12.8. TLC and IR indicated that these complexes were formed by electrostatic interaction between opposite charges. The complexes had different solubility characteristics from their individual components. They were solubilized in the palisade layer of surfactant micelles, exhibited unusual surface tension–concentration and turbidity–concentration curves, and slowly precipitated from aqueous solution with time. A microscopic investigation showed that this "precipitation" was in fact a coacervation phenomenon, and the unusual behavior of the interaction product was attributed to the formation of a complex coacervate.

Coacervate droplets were also formed when dilute aqueous solutions of surfactant and dye were mixed, but floccules formed at high concentrations; at very high concentrations, some viscoelastic systems were observed. A simple viscometric investigation of these systems showed that the specific viscosity increased sharply as the ratio of dye to surfactant increased up to the point where the system coacervated. It was also shown that surfactant micelles are not necessary for interaction to occur between dye and surfactant. Viscosities for solutions of long-chain surfactants with dye were higher than those with short-chain surfactants.

Coacervate droplets exhibited the typical behavior of coacervates in an electric field, *i.e.*, electrophoresis, deformation, and disintegration.

The incompatibility of amaranth and alkyltrimethylammonium salts to form a coacervate in aqueous solution was investigated by phase study titrations. The minimum ratio of surfactant to dye for compatibility (or for coacervation to be just suppressed) was found to depend on a number of factors: the alkyl chain length of the surfactant, the concentration of reactants present in solution, pH, temperature, and the concentration and valency of added salt. Results were interpreted using the general coacervation theories of Bungenberg de Jong (27) and Voorn (40).

The compatibility of dyes with surfactants is important in the formulation of pharmaceutical products. Surfactants are used extensively to solubilize volatile oils, vitamins, hormones, and other water-insoluble drugs and it is likely that such systems also contain a dye as colorant. A thorough investigation of such incompatibilities as discussed in this paper can be valuable to the research pharmacist in the formulation of liquid preparations, particularly those containing solubilized drugs.

REFERENCES

(1) J. Swarbrick, *J. Pharm. Sci.*, **54,** 1229(1965).

(2) W. U. Malik and S. P. Verma, *J. Amer. Oil Chem. Soc.*, **44,** 46(1967).

(3) W. U. Malik and S. P. Verma, *J. Phys. Chem.*, **67,** 2082 (1963).

(4) B. R. Craven and A. Datyner, *J. Soc. Dyers Colour.*, **83,** 41 (1967).

(5) *Ibid.*, **77,** 304(1961).

(6) *Ibid.*, **79,** 515(1963).

(7) G. Zografi, P. R. Patel, and N. D. Weiner, *J. Pharm. Sci.*, **53,** 544(1964).

(8) M. Hayashi, *Bull. Chem. Soc. Jap.*, **34,** 119(1961).

(9) K. Tori and T. Nakagawa, *Kolloid-Z.*, **191,** 42(1963).

(10) A. Badinand and J. Guiraud, *Trav. Soc. Pharm. Montpellier*, **14,** 119(1954).

(11) P. Mukerjee and K. J. Mysels, *J. Amer. Chem. Soc.*, **77,** 2937(1955).

(12) C. W. Ballard, J. Isaacs, and P. G. W. Scott, *J. Pharm. Pharmacol.*, **6**, 971(1954).
(13) L. Lachman, R. Kuramoto, and J. Cooper, *J. Amer. Pharm. Ass., Sci. Ed.*, **47**, 871(1958).
(14) E. L. Colichman, *J. Amer. Chem. Soc.*, **73**, 1795(1951).
(15) *Ibid.*, **72**, 1834(1950).
(16) *Ibid.*, **73**, 3385(1951).
(17) H. B. Klevens, *J. Phys. Chem.*, **51**, 1143(1947).
(18) L. D. Metcalfe, *J. Amer. Oil Chem. Soc.*, **40**, 25(1963).
(19) B. W. Barry, J. C. Morrison, and G. F. J. Russell, *J. Colloid Interface Sci.*, **33**, 554(1970).
(20) B. W. Barry and G. M. Saunders, *J. Pharm. Sci.*, **60**, 645 (1971).
(21) M. Donbrow, "Instrumental Methods in Analytical Chemistry," vol. 1, 1st ed., Pitman & Sons Ltd., London, England, 1967.
(22) A. V. Few and R. M. Ottewill, *J. Colloid Sci.*, **11**, 34(1956).
(23) S. Riegelman, N. A. Allawala, M. K. Hrenoff, and L. A. Strait, *ibid.*, **13**, 208(1958).
(24) J. P. Kratohvil, M. Kerker, and L. Oppenheimer, *J. Chem. Phys.*, **43**, 914(1965).
(25) H. A. Abramson, L. S. Moyer, and M. H. Gorin, "Electrophoresis of Proteins," Reinhold, New York, N. Y., 1942.
(26) M. Von Smoluchowski, *Z. Phys. Chem.*, **92**, 129(1917).
(27) H. G. Bungenberg de Jong, in "Colloid Science," vol. II, H. R. Kruyt, Ed., Elsevier, New York, N. Y., 1949.
(28) M. E. Auerbach, *Ind. Eng. Chem., Anal. Ed.*, **15**, 492(1943).
(29) S. Riegelman, *J. Amer. Pharm. Ass., Sci. Ed.*, **49**, 339(1960).
(30) H. G. Bungenberg de Jong and H. R. Kruyt, *Proc. Kon. Ned. Akad. Wetensch.*, **32**, 849(1929).
(31) H. G. Bungenberg de Jong and H. R. Kruyt, *Kolloid-Z.*, **50**, 39(1930).
(32) A. Kossel, "The Protamines and Histones," Longmans, Green & Co., London, England, 1928.
(33) H. Stendel and E. Peiser, *Z. Physiol. Chem.*, **122**, 292(1922).
(34) H. G. Bungenberg de Jong and W. A. L. Dekker, *Kolloid-chem. Beih.*, **43**, 143(1935); *ibid.*, **43**, 213(1936).
(35) H. G. Bungenberg de Jong and R. F. Westerkamp, *Biochem. Z.*, **234**, 347(1931).
(36) E. H. Büchner and A. H. H. Van Royen, *Kolloid-Z.*, **49**, 249 (1929).
(37) H. P. Frank, *J. Colloid Sci.*, **12**, 480(1957).
(38) B. Milicevic, *Proc. Int. Congr. Surface Active Substances, 4th, Brussels*, **1964**, 577.
(39) H. G. Bungenberg de Jong and P. H. Tennissen, *Kolloid-Beih.*, **47**, 254(1938).
(40) M. J. Voorn, *Rec. Trav. Chim.*, **75**, 317, 405, 427, 925, 1021 (1956).
(41) P. Debye and E. Hückel, *Phys. Z.*, **24**, 185(1923).
(42) P. J. Flory, *J. Chem. Phys.*, **10**, 51(1942); *ibid.*, **12**, 425(1944).
(43) H. Eisenberg and G. R. Kohan, *J. Phys. Chem.*, **63**, 671 (1959).
(44) A. Katchalsky and H. Eisenberg, *J. Polym. Sci.*, **6**, 145 (1951).
(45) W. B. Hardy, *Proc. Roy. Soc. London*, **66**, 110(1900).
(46) H. Schulze, *J. Prakt. Chem.*, **25**, 431(1882).
(47) J. T. G. Overbeek and M. J. Voorn, *J. Cell. Comp. Physiol.*, **49**, 7(1957).
(48) L. S. C. Wan, *J. Pharm. Sci.*, **55**, 1395(1966).
(49) *Ibid.*, **56**, 743(1967).
(50) *Ibid.*, **57**, 1903(1968).
(51) H. P. Frank, S. Barkin, and F. R. Eirich, *J. Phys. Chem.*, **61**, 1375(1957).

ACKNOWLEDGMENTS AND ADDRESSES

Received June 29, 1970, from the *School of Pharmacy, Portsmouth Polytechnic, Portsmouth PO1 2DZ, England.*

Accepted for publication December 20, 1971.

* Present address: Organon Laboratories, Ltd., Newhouse, Lanarkshire, Scotland.

▲ To whom inquiries should be directed.

Pharmacokinetics of Three Sulfonamides in the Rabbit

KERRY ANN McMAHON and W. J. O'REILLY▲

Abstract □ The blood level–time relationships for sulfamethazine, sulfisomidine, and sulfathiazole were determined in rabbits after intravenous injection. The results were fitted to a two-compartment open model, and the parameters and rate constants for the model were obtained. Differences between drugs, animals, and treatments (water loading) were studied in terms of urinary and metabolic rate constants, intercompartment diffusion constants, and clearance values. Sulfisomidine was the most slowly eliminated of the compounds, mainly because of the rabbit's low capacity to metabolize this compound. Water loading increased the fraction of drug excreted free (f). It reduced the k_m for sulfathiazole but produced no change with the other drugs. The clearances of the compounds from the central compartment were calculated using $V_b \cdot k_u$ as the apparent renal clearance and $V_b \cdot k_m$ as the metabolic clearance. The apparent renal clearance calculated for all drugs was increased by water loading, while the metabolic clearance was unaffected. The metabolic clearance was suggested as a useful basis for quantitative comparison of the metabolism of these drugs.

Keyphrases □ Pharmacokinetics, sulfamethazine, sulfisomidine, sulfathiazole—after intravenous administration, rabbits □ Sulfamethazine—blood level–time relationships after intravenous administration, pharmacokinetic parameters, rate constants, rabbits □ Sulfisomidine—blood level–time relationships after intravenous administration, pharmacokinetic parameters, rate constants, rabbits □ Sulfathiazole—blood level–time relationships after intravenous administration, pharmacokinetic parameters, rate constants, rabbits

One of the most important factors regulating the response of an organism to a drug or toxic agent is the rate at which the compound is eliminated from the body. Williams (1) pointed out that the main difference between man and animals in drug response probably lies in the varying abilities of different species to carry out drug metabolism. Therefore, a knowledge of comparative pharmacokinetics should be useful in both pharmacology and toxicology. In this paper, sulfonamides are used as model compounds to explore the